A PALEODEMOGRAPHIC STUDY OF MORTALITY IN 1ST CENTURY BC/AD PETRA, JORDAN

By

Akacia Propst

July, 2017

Director of Thesis: Dr. Megan Perry

Major Department: Anthropology

The 1st century BC to 1st century AD population of Petra appears to have rarely suffered from infectious diseases based on the low frequency of pathological bone lesions in skeletons recovered from tombs on the site's North Ridge. However, many infectious diseases in the past killed their hosts before a skeletal lesion could form, rendering their effects essentially invisible in ancient populations. Cemetery-level age-at-death profiles can provide an important supplementary record of disease-related mortality by distinguishing between samples created by catastrophic events, such as disease epidemics, versus a normal attritional cemetery sample that accumulates over time. Here, age-at-death estimates for 70 individuals, out of a current MNI of 120, were estimated using cementochronology, which not only provides more accurate age estimates, but increases our sample size of ageable individuals limited by the fragmented and commingled nature of the Petra assemblage. A Gompertz-Makeham hazard model was used to calculate mortality risk by age in this sample. The age-at-death results and the results from the parametric hazard modeling suggest that mortality peaked for the North Ridge population around the age of 50-55 and that they experienced relatively low age-specific risk of mortality for a pre-industrial, urban population. When compared to the contemporaneous population of Isola Sacra, the results indicate a

significant difference in age-specific mortality between the North Ridge population and Isola Sacra where the North Ridge population has a significantly lower age-specific mortality risk. A comparison of these two populations suggest that the political-economic environment, nutritionally adequate diet, the urban environment, and regional demography culminated in low prevalence of paleopathological conditions and may begin to explain the relatively low age-specific mortality risk for this population.

A PALEODEMOGRAPHIC STUDY OF MORTALITY IN 1ST CENTURY BC/AD PETRA, JORDAN

A Thesis Presented to the Faculty of the Department of Anthropology
East Carolina University

In Partial Fulfillment of the Requirements of the Degree of

Masters of Arts in Anthropology

Summer 2017

by

Akacia Propst

A PALEODEMOGRAPHIC STUDY OF MORTALITY IN I ST CENTURY BC/AD PETRA, JORDAN

by

Akacia Propst

APPROVED BY:

DIRECTOR OF THESIS: _____
Megan Perry, PhD

COMMITTEE MEMBER: _____
Benjamin Saidel, PhD

COMMITTEE MEMBER: _____
Blakely Brooks, PhD

CHAIR OF THE DEPARTMENT
OF ANTHROPOLOGY: _____
Randolph Daniel, PhD

DEAN OF THE
GRADUATE SCHOOL: _____
Paul J. Gemperline, PhD

ACKNOWLEGEMENTS

I would like to thank my adviser, Dr. Megan Perry, for the opportunity to do this project and for her guidance and assistance throughout its development. I would also like to thank my committee members Dr. Benjamin Saidel and Dr. Bailey Brooks for their insightful input on the written portion of this project. I would also like to thank Dr. Sharon DeWitte for her instruction and guidance with the parametric hazard modeling. Without her instruction on and sharing of the mle programs and the application of the Gompertz-Makeham formulas the parametric hazard modeling and statistical analysis would not have been possible. I would like to thanks my friend and family whose support helped make this work possible. I would like to thank ACOR and ASOR for the financial support helped make my participation in the Petra North Ridge Project and the project possible. I would also like to thank all funding institutions that provided the resources that made this project possible.

TABLE OF CONTENTS

LIST OF TABLES

LIST OF FIGURES

Chapter 1: Introduction

Petra, the political center of the Nabatean kingdom now located in modern day Jordan, flourished during the 1st century BC to the 1st century AD. The Nabataean kingdom would come to span from southern Syria to Northern Saudi Arabia and West across the Negev desert into modern day Israel (Al-Salameen 2011). Diodorus describes the Nabataeans in the 4th century BC as skillful nomadic traders whose laws prevented building permanent homes (*Library of History* 19.94.1; 95.1-97.6). By the 1st century BC, the Nabataeans had changed dramatically. During this period, Strabo describes the Nabataeans as having developed an established monarchy, lavish houses, and possessing luxurious goods (*Geography* 16.4.27; Oleson 2007). The landscape of the Nabataean kingdom and Petra had also changed drastically. Large monumental structures were being built throughout Petra, including the large façade tombs that now define its landscape.

Due to the sparseness of historical records written about or by the Nabataeans, archaeological research is responsible for building much of what we know about Petra and the Nabataean Kingdom. However, other fields of research such as bioarchaeology allow us to reconstruct the lived experience of Petra's inhabitants and examine how they navigated and experienced their urban environment. One way to measure this is through mortality. Mortality risk is the outcome of many factors that work congruently with one another. Therefore, mortality risk is both the outcome and reflective of the larger socio-political environments in which populations lived and is informative about how successfully or unsuccessfully these populations maneuvered and adapted to their environments.

The purpose of this study is to create a mortality profile for the Petra North Ridge population. The commingled and fragmented nature of the skeletal remains recovered from the

North Ridge tombs has made this difficult in the past using standard bioarchaeological methods of age estimation. In this study, I use cementochronology and parametric hazard modeling to estimate the age-at-death and the age-specific risk of mortality for 70 individuals recovered from 6 tombs on Petra's North Ridge dating to the 1st century BC to the 1st century AD. In order to contextualize the results from Petra, I will compare them with bioarchaeological study of skeletal remains from another important trading center closer to the imperial center of Rome, that of Portus in Italy.

The aim of this study was three-fold. First, to clarify the paleopathological data previously collected for this non-elite population by determining whether or not it is indicative of a normal cemetery sample or one that suffered from virulent disease. This can be done by using the age-at-death estimates to model the distribution of mortality for Petra's non-elite. Second, to estimate the age-specific risk of mortality to determine the rates of mortality among the North Ridge population, how it compares to other contemporaneous populations, and how this data might be used to better understand the social and physical environments the North Ridge populations resided in. Third, to understand how social, cultural, and political factors effected mortality risk among Petra's non-elite by drawing on epidemiological and medical anthropological models of health in conjunction with archaeological and historical data for Petra and the broader Nabataean kingdom, in addition to Portus and its Roman imperial context.

Chapter 2 provides the historical background of the Nabataean kingdom and Petra and previous bioarchaeological research on Petra's non-elite. Following this is a background on the methods used in this analysis including the use of cementochronology in bioarchaeological research, parametric hazard modeling in paleodemography, and a review on how these methods are applied to the sample. Following this is a brief discussion on how this study builds upon previous research and contributes more to our understanding of this population. Chapter 3 outlines

the methodology employed to retrieve and analyze the data. This includes cementochronology, the construction of a traditional life table, parametric hazard modeling, and an analysis of differential mortality.

Chapter 4 discusses the results of the age-at-death estimates derived through cementochronology including the age-at-death distribution of the North Ridge population and how it compares to other contemporaneous populations. The results of the parametric hazard modeling are compared to those derived from the life table and then evaluated against another ancient, urban population. Chapter 5 delves into a comparison of the North Ridge population to the population of Portus in order to highlight the variables that led to differing patterns of age-specific mortality risk. Chapter 6 summarizes the findings, highlights how mortality contributes to our understanding of Petra's non-elite when considered in the context of the paleopathological and dietary data for Petra, and the significance of the data within the broader framework of our understanding of mortality in pre-industrial, urban populations. Finally, future avenues of research are discussed as they relate to the paleodemographic profile of Petra's non-elite population.

Chapter 2: Background

The expedition of Johann Ludwig Burckhardt in 1812 to Wadi Musa marked the rediscovery of the rose red city of Petra to the western world. Following shortly afterwards, J.L Burckhardt's account of Petra inspired other explorers to study and document the landscape of the ancient city. Although never lost to the locals, this "rediscovery" spawned a new awareness of Petra and the Nabataean Kingdom throughout the western world. In the years since, decades of archaeological and historical research have contributed greatly to a more expansive and nuanced understanding of the Nabataeans, their kingdom, and their role in history.

Historical Background

The early history of the Nabataeans remains largely unclear. Beginning in the 4th century BC, groups of nomadic Arabs began to migrate into the area that would come to be known as Nabataea (Schmid, 2008; Wenning, 2007). Where exactly these groups migrated from remains contested. It is most often assumed, however, that they migrated north from the Arabian Desert and eventually coalesced with the local populations in the region (Bowersock 2003; Parr 2003). As these nomadic groups migrated to this region, they gradually assumed a prominent commercial role in the area as middlemen in the incense trade (Bowersock 2003).

Due to their nomadic nature, there is little material culture to speak of the lives or origins of these early groups. The primary source for this period of Nabataean history is Diodorus' work *Library of History*, written in the 1st century BC (19.19-100; 2.48-49). In this account, Diodorus depicts early Nabateans as skillful nomadic traders between South Arabia and the Syro-Phoenician coast (*Library of History* 19.94.1; 95.1-97.6). He also makes reference to a rocky stronghold where the Nabataeans left behind their families and goods during trade and other business. Some have

Figure 1: Map of modern day Jordan marking the location of Petra.

asserted that the description of the rocky stronghold resembles the landscape surrounding Petra and attests to Petra's early function as a center for the Nabataeans (Schmid 2008).

The 2nd century BC marked the decline of the Seleucid dynasty in the ancient Near East, setting off a chain of events that led to an increase in long-distance trade throughout the region which may have subsequently encouraged the Nabataeans to become more sedentary. During this period, two centuries after the presumed migration of Nabataeans into the region, the first definitive evidence of a uniquely Nabataean material culture appears in the archaeological record. These items show a strong influence of the mainstream forms and styles of the contemporary Hellenistic world as represented in the Near East. The presence of this material culture where there

had been little to none before suggests that a process of sedentarization had begun during this period (Schmid 2008).

By the 1st century BC, the material culture of the Nabataeans developed rapidly to include major architectural complexes and monumental façade tombs (Schmid 2008). We see a trend towards monumentalization in the construction of houses that represent clear social differentiation, temples, water systems, and monumental façade tombs (Schmid 2008). A distinctive Nabataean material culture develops during this period, particularly in pottery and numismatics (Schmid 2008; Wenning 2007).

This was also a period of increasing Nabataean presence in the Near East. Nabataean material culture, such as coins, inscriptions, and similar architecture, are found in areas throughout the regions outside Nabataea (Al-Salameen 2011). Archaeological evidence even suggests that there might have been direct contact as far as India (Gogte 1999). The Nabataean Kingdom itself expanded to cover a wide geographical area from southern Syria to Northern Saudi Arabia and West across the Negev desert into modern day Israel (Al-Salameen 2011).

Strabo's *Geography* (16.4.24-27) is the primary written historical source for this period. Written before 3/2 BC, Strabo describes the Nabataeans of this century as having an established monarchy, small-scale urbanism that included lavish houses, agriculture, diverse herds of animals, and extravagant possessions obtained through manufacture and long-distance trade (Oleson 2007: 219; Wenning 2007). Additionally, he writes of a thriving diverse community distinguishable for the number of foreigners present at Petra.

Throughout Nabataean history, one of the main sources of wealth for the Nabataean Kingdom were trade activities, especially the incense trade (Bowersock 2003; Schmid 2008). The

Nabataeans controlled and monopolized incense trade routes that connected Arabia with the larger Mediterranean region (Al-Salameen 2011) The primary two commodities traded along this route included frankincense and myrrh (Al-Salameen 2011). Located at the center of these trade routes was Petra, the economic and political center of the Nabataean Kingdom. By the beginning of the 1st century AD, Petra was not just a major trade hub but also an important center of production for valuable luxury goods such as unguents, incense, and amethyst beads (Johnson 1987).

The historical development of Petra follows the major developments of the Nabatean kingdom. Indeed, sedentarization of parts of Nabataean society is generally understood as beginning when Petra was selected as the seat of head tribal figures (Wenning 2007). The initial development of Petra has proved to be somewhat elusive, however. The lack of inscriptions on buildings has left pottery and numismatic data as the primary archaeological evidence to date these buildings. Some of the earliest free-standing structure at Petra to be confidently dated consist of walls located under the Colonnaded Street that runs through the center of Petra. Using numismatic evidence, this structure was dated to the reign of Aretas II (c. 100-96/92BC; Parr 2007). Further excavations by Graf et al. (2005) in this area successfully revealed pre-100BC structures firmly dated to the early-Hellenistic era (3rd-2nd century BC). Radiocarbon dating further indicates occupation in Petra as early as 790-420 BC, suggesting a long history of habitation.

It is not until the mid-1st century BC that the first indications of monumental architecture indicating Petra's city status appears in the archaeological record. By the last quarter of the 1st century BC important building activities of monumental structures, such as Qasr al-Bint and the monumental façade tombs so characteristic of Petra, begin increasing (Schmid 2008). Throughout these periods, the Romans were becoming more influential and exerting a greater presence in the Near East. By the beginning of the 1st century AD the Roman empire officially bordered the

Nabataean kingdom with the creation of the province *Judaea* to the west (Millar 1993). The Romans' increasing influence is attested to by the Nabataeans when Aretas IV (9 BC – 40 AD) sent ambassadors to Rome. This visit was commemorated on a marble inscription on the Capitoline, suggesting that at this time Nabataea served as a Roman client kingdom in the Near East (Bowersock 2003).

In 106 AD, the Romans officially annexed the Nabataean Kingdom as the Roman province of *Arabia*. After Roman annexation, a contraction in city size took place and a new city wall was built (Parker 2016; Parr 2007). Although life does not appear to have changed substantially following Roman annexation, a distinctly Nabataean contribution to life in *Provincia Arabia* becomes increasingly difficult to parse out in the historical and archaeological record as time passes. Evidence for the Roman military and administrative presence instead begins to proliferate (Bowersock 2003).

Today, the ruins of the city are surrounded by sandstone cliffs containing the Nabataean's monumental funerary structures, a central focus for researchers and tourists alike (Anderson 2002; Schmid 2008; Wadeson 2012). However, these are only one of four main types of tombs that can be found in Petra: façade tombs, cuboidal tombs, shaft tombs, and pit tombs (Wadeson 2012). The façade tombs at Petra are cut into the bed-rock of cliffs with a façade carved around the entrance (Wadeson 2012). The interiors of these structures are usually comprised of square-shaped chambers with grave shafts or loculi carved into the floors and walls for burials (Wadeson 2012). Most also have exterior platforms that were built for funerary feasting and other rituals (Wadeson 2012). Some have simple exterior structures such as basins and niches while others have extensive funerary complexes composed of porticoes, triclinia, benches, and cisterns (Wadeson 2012). These tombs where primarily constructed during Petra's height in the 1st century BC to the 1st century

AD (Wadeson 2012). Block tombs consist of free form structures that stand separate from the bedrock they were carved from (Wadeson 2012). There are only 6 known in the whole of Petra and they represent some of the earliest monumental tombs (Mouton 2006; Sachet 2005). They are primarily located at entrances to the city and in areas where the sandstone is not suitable for façade tombs (Wadeson 2012).

Less well known are the pit and shaft tombs, of which there are more than 800 in Petra (Wadeson 2012). The pit graves are simple, rectangular graves constructed for one or several burials (Wadeson 2012). The shaft tombs consist of shafts cut down into the bedrock, rather than cliff sides like the façade tombs. These shaft tombs often have a ~3m shaft descending down in the bedrock that open up to a roughly square shaped chamber. Within this chamber, pit graves and loculi are carved into the floor and walls for burials. Where the façade tombs are thought to represent the burials of elite individuals at Petra, the pit graves and shaft tombs most likely represent individuals and communities from the non-elite socio-economic classes (Bikai and Perry 2001; Parker and Perry 2013; Perry 2002; Perry 2015). With the proliferation of tomb structures throughout the landscape, Petra is certainly not lacking in human skeletal remains.

However, the skeletal remains of Petra's past inhabitants represent an often-overlooked resource for understanding life in Petra. Bioarchaeological research on human skeletal samples affords the opportunity to study many facets of life in Petra that are difficult to reconstruct from archaeological material alone (see Larsen 2015). This includes the presence and prevalence of infectious diseases, degenerative conditions, and chronic physical stress experienced by a population; relatedness of populations through metric and non-metric traits; population structure including patterns of mortality, morbidity, and fertility through age-at-death estimates; and physical activity patterns through skeletal markers. Bioarchaeological research also contributes

greatly to archaeological studies on migration and diet through stable isotopic analysis (White et al. 2012). As such, data derived from analyses on human skeletal remains represent an important resource for understanding the lifeways and environments of Petra's population.

Despite the abundance of tombs and skeletal materials, the discovery and recovery of human skeletal remains during excavations of these structures have been largely incidental rather than deliberate, and little or no mention of basic biological information, such as age and sex, have been provided in published reports (Perry 2016). Currently, the Petra North Ridge Project (PNRP) represents one of the only systematic excavations of Nabataean skeletal remains and bioarchaeological research in Petra. The Petra North Ridge Project includes the excavation of Nabataean shaft-tombs and the neighboring domestic structures located along Petra's North Ridge (Parker 2016; Parker and Perry 2013; Perry 2016). The shaft tombs were in use from the 1st century BC to the 1st century AD. As of 2016, seven shaft tombs have been completely excavated. The skeletal assemblage from these tombs allows for insight into the lifeways of Petra's common citizenry whose presence is less visible among the monumental façade tombs and buildings.

Previous research on the PNRP collection including diet and paleopathology have already provided great insight about Petra's non-elite population. Appleton's (Appleton 2015) analysis of diet using stable carbon and nitrogen isotopes revealed that the PNRP population had a rather complete diet composed primarily of foods like wheat, lentils, olives, and figs in addition to healthy amounts of proteins and lipids from animals. This analysis discovered a marked difference in carbon values between the individuals in Tomb 2, recovered during a previous excavation of the North Ridge Church, and the remains from tomb B4 and B5. Additionally, the individuals in B4 and B5 exhibited a lesser degree of dietary variation than those in Tomb 2. Appleton (2015)

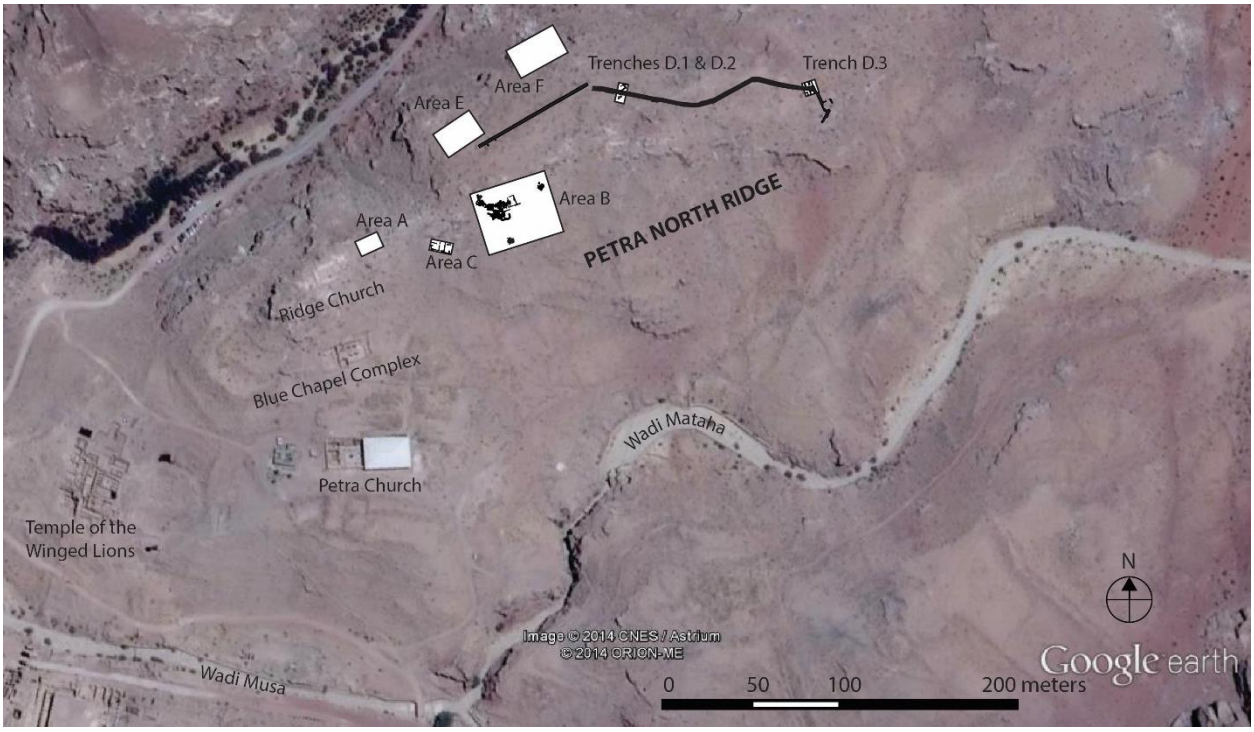

Figure 2: Map of the North Ridge in Petra. The shaft tombs excavated in 2012, 2014, and 2016 field seasons are located in Area B and Area F. Tombs 1 and 2 from the 1999 season are located by the Petra Church.

surmises that this variability in diet may be due to different food preferences of extended families. Or, the family represented in Tomb 2 may have had access to more resources, and thus a greater variety of food, than those from tombs B4 and B5.

In her paleopathological analysis, Canipe (2014) recorded the presence and prevalence of periostitis, cribra orbitalia, porotic hyperostosis, linear enamel hypoplasia, osteoarthritis, vertebral osteophytosis, osteoporosis, and trauma among the PNRP remains excavated in 2012 to better understand disease and physiological stress in this population. Periostitis, the inflammation of the bone periosteum, is a non-specific indicator of general infection (Ortner 2003). Cribra orbitalia and porotic hyperostosis result from the outward expansion of the inner trabecular bone, resulting in a pocked or porous appearance on the inside of the eye sockets and cranial vault respectively

(Ortner 2003). These conditions have been connected to iron or B_{12} deficiencies which can stem from malnutrition and disease (Ortner 2003; Walker et al. 2009). Linear enamel hypoplasia is a dental defect caused by the disruption of enamel formation resulting in grooves and pits on the enamel (Ortner 2003). Like periostitis, enamel hypoplasias are a result of general non-specific physiological or psychological stress during childhood (Goodman et al. 1988; Ortner 2003). In contrast, vertebral osteophytosis, osteoarthritis, and osteoporosis are degenerative conditions linked to activity patterns and aging (Ortner 2003).

The results of this analysis revealed that Petra's non-elite suffered primarily from degenerative diseases represented by osteoarthritis and vertebral osteophytosis. Canipe (2014) concludes that the low prevalence of periostitis among the Petra population in relation to other agricultural and rural/nomadic populations from the region could suggest that related conditions, such as infectious disease and malnutrition, were not prevalent in Petra. The complete lack of both porotic hyperostosis and cribra orbitalia further complemented these results. Moreover, levels of enamel hypoplasia among the PNRP population were similar to those seen in contemporaneous rural/nomadic settlements and were significantly lower compared to other urban populations. This is contrary to what is expected for pre-industrial, urban populations. Namely, they tend to exhibit more indicators of poor health due to environmental conditions associated with urbanism, compared to rural or nomadic populations (Larsen 2015). However, these results do not rule out the possibility that Petra's non-elite suffered from virulent infectious diseases that resulted in death before bony responses could form.

Canipe's (2014) findings were consistent with the results of previous research on a Nabataean non-elite human skeletal sample. During the 1999 excavation of the North Ridge Church, two Nabataean shaft tombs dating to the first century AD were recovered (Bikai and Perry

2001). Examination of these remains revealed similar low levels of paleopathological markers related to infectious disease and malnutrition, and a greater prevalence of degenerative diseases. Tomb 2 in particular offered insight into the life history of an extended Nabatean family who lived in the first century AD. These individuals appear to have led healthy, active lives. Like the individuals excavated later on, they exhibited few indicators of stress or chronic disease but would come to experience age-related degenerative conditions, such as vertebral osteophytosis and degenerative joint disease, as they got older.

Age-at Death Estimations and Paleodemography

Building a mortality profile for the North Ridge population allows us to better interpret and understand previous research on diet and physical stress. To do so, the age-at-death of individuals in the skeletal assemblage must be estimated. Traditional methods for establishing age-at-death rely upon developmental and degenerative markers. For sub-adults, typically defined as individuals who have not reached full skeletal development, developmental markers such as tooth eruption and epiphyseal fusion allow for fairly accurate age-at-death estimations. For adults, however, there is a much larger margin of error because degeneration, such as the wear of the pubic symphysis and auricular surface on the pelvis, are more variable between individuals and much more subject to environmental conditions (Bocquet-Appel and Masset 1982; Chamberlain 2006). Due to this, accurately determining the age of older individuals is much more difficult.

Issues with estimating the age of adults poses particular difficulties for paleodemographic reconstructions of ancient populations. Bocquet-Appel and Masset (1982) compared age estimates using six different skeletal elements for aging adults and found a maximum correlation of $r = 0.829$ for males and $r = 0.794$ for females. At this level of correlation, they estimate that there can be errors as high as 29 years when determining age-at-death for adults within a 95% confidence range.

Errors as large as these can significantly skew paleodemographic models. Indeed, in archaeological samples under-aging of older individuals is a common issue and often results in paleodemographic profiles that would appear to show that few individuals lived beyond 60 years of age (Bocquet-Appel and Masset 1982; Chamberlain 2006). This, however, does not correlate well with historic populations for which we have census records, indicating that this is a product of under-aging rather than historical reality in many cases (Bocquet-Appel and Masset 1982).

Additionally, age-at-death estimates can be further biased by mirroring reference samples. Reference samples used to develop age estimation techniques rely on observing changes in skeletal indicators by age in human skeletal collections with known ages at death. However, if a reference sample does not have an even age distribution, there will be less data available for underrepresented age groups. Any use of this method to estimate the age of individuals in an archaeological population will result in many individuals being placed into the age categories for which there was greater representation in the reference population. This can then result in an age-at-death distribution for archaeological samples that mimics that of the reference population (Bocquet-Appel and Masset 1982; Chamberlain 2000, 2006; Milner et al. 2008). Together, these biases have resulted in difficulties for producing reliable age-at-death estimates and paleodemographic models of mortality and fertility for ancient populations. This has indeed led some to argue that age-at-death estimates should not be used for anything but general inferences about historical populations (Bocquet-Appel and Masset 1982).

Cementochronology

Recent paleodemographic research has focused creating new techniques and methods that might help remediate the paleodemographic biases described above and new age estimation methods that provide a more precise indicator of age have been developed. One such method is

cementochronology. This method uses the cementum covering the tooth root as an indicator of age. Originally developed to produce age estimation for animals, Stott et al. (1982) determined that cementochronology could be successfully applied to humans. Since then, cementochronology's value as a method for estimating age-at-death in archaeological populations has begun to be realized in bioarchaeological studies (Charles et al. 1986; Schug et al. 2012).

The cementum's primary function is to anchor collagen fibers of the periodontal ligament to the root surface of the tooth and keep the tooth in a stable position throughout life (Naji et al. 2016). There are three different types of cementum that form the overall cementum layer: acellular extrinsic fibers, cellular intrinsic fibers, and cellular mixed stratified (Naji et al. 2016). Cellular cementum is a reactive tissue that is characterized by periodic, irregular growth in response to physical stress (Naji et al. 2016). Acellular cementum, on the other hand, has a regular growth cycle that results in the deposition of one light band of cementum and one dark band of cementum every year (Charles et al. 1986; Naji et al. 2016; Wittwer-Backofen et al. 2004). Cementum apposition begins when the tooth is about to reach the occlusal level and erupt (Bosshardt and Selvig 2000). By totaling the numbers of light and dark bands and adding this to the average age of tooth eruption, a very precise age-at-death figure can be estimated.

Unlike common aging methods that measure the stage of development or the level of degeneration of skeletal elements (Buikstra and Ubelaker 1994), cementochronology is currently one of the only age indicator in bioarchaeology that uses a reliable and continuously growing tissue (Naji et al. 2016). Research testing the accuracy of cementochronology for age-at-death estimations have, overall, produced very promising results. The average correlation between known age and estimates using cementochronology in over 16 validation studies is $r = 0.87$, 10 of which had correlation rates above $r = 0.90$ and only 4 with correlations below $r = 0.80$ (Naji et al.

2016). Within a 95% confidence interval, an accuracy rate of ± 2 year has been achieved with cementochronology. In contrast, traditional aging methods have an average accuracy rate of ± 5 years, which increases dramatically the older an individual is (Charles et al. 1986; Wittwer-Backofen et al. 2004).

Other studies have shown a slightly weaker, but still relatively strong correlation between cementochronology and known age for individuals in older age categories, which have notoriously high error rates when using standard methods. Stein and Corcoran (1994) calculated a correlation coefficient of r = 0.98 for individuals younger than 60 and a correlation coefficient of r = 0.85 for individuals over 60. They posited that this is due to a decrease in cementum apposition in older individuals, which can diminish by up to one-third after the age of 60. Additionally, conditions such as periodontal disease may damage the cementum and lead to less reliable age-at-death estimates (Naji et al. 2016). However, Wittwer-Backofen et al. (2004) found minimal effects of age-related differences and dental diseases in their validation study using teeth from individuals of known ages. They suggest that it is the methods and equipment used, as well as the condition of the teeth themselves, that cause decreased correlation rather than any inherent effects of age or dental pathology. In particular, the older an individual is, the more bands of cementum there are to count, which can lead to a greater probability of intraobserver error.

Parametric Hazard Modeling

Due to the nature of the skeletal samples that paleodemographic data is based upon, the data also suffers from a number of sample related issues that can introduce bias. These include sampling bias, infant underenumeration, small sample sizes, and differential preservation (Chamberlain 2006). As a result, a mortality profile developed from the sample will not accurately reflect the actual age-related pattern of mortality at the site. However, the use of mathematical

modeling, such as parametric hazard models, can help correct for the biases inherent in every skeletal assemblage.

Hazard models are used in many disciplines to compute the probability of a "hazard" occurring at a specific time or age. For mortality, parametric hazard models work by reducing the age categories in traditional life tables to a small number of biologically meaningful parameters that can then be estimated from age-at-death estimates (Gage 1989; Gage and Dyke 1986; Gavrilov and Gavrilova 1991); Wood et al. 2002: 143). It has not been until the past few decades that parametric hazard models have begun to be widely applied in demographic research as advances in computer technology have facilitated their use (Mode and Busby 1984; Mode and Jacobsen 1984; Wood et al. 1992, 2002: 143). In palaeodemographic studies, parametric hazard analyses are used to calculate the probability of death occurring at a specific age and have distinct advantages when modeling mortality. Parametric hazard analysis smooths out mortality models and fills in the gaps in the data due to small sample size and sampling bias without imposing specific patterns of mortality on the population being studied (Wood et al. 2002). They do so by applying parameters that model a basic distribution of human mortality risk that remains broad enough that it does not impose itself upon the raw data (Wood et al. 2002).

The parametric hazard models most often used for estimating the age-specific risk of mortality include the Gompertz, the Gompertz-Makeham, and the Siler model. Benjamin Gompertz first formulated the Gompertz model in the early 1800s (Gompertz 1825). This model was created on the basic assumption that human mortality risk increases exponentially with age. As such, the Gompertz model consists of two parameters that model the increased risk of mortality with age in order to estimate mortality risk (Wood et al. 2002).

The Gompertz-Makeham model was created as an improvement to the basic Gompertz model by William Makeham in the 1860s (Makeham 1860). Makeham added another parameter to the two parameter Gompertz model, known as the Makeham component. This component models for age-independent risks of mortality and incorporates mortality related to accidents that can create a "hump" in mortality during the late-teens and early twenties in modern populations. This model has been proven to better fit patterns of human mortality risk than the Gompertz model alone. However, the Makeham component is often very difficult to calculate in paleodemographic populations due to small sample sizes (Wood et al. 2002).

W. Siler created the Siler model in the 1970s in order to study mortality in animals (Siler 1979). This model consists of the Gompertz-Makeham model with the addition of one more component consisting of two parameters, known as the immature component, which model's mortality at the time of birth and throughout childhood. By adding this component, the age-specific risk of mortality can be estimated across the entirety of the human life-span. Validation studies on the efficacy of the Siler model have revealed that it fits better than other parametric hazard models and that it provides a good fit for a range of different age patterns of mortality (Gage 1988).

Parametric hazard modeling also has a number of advantages over model life-tables, a traditional staple in paleodemographic studies. Model life tables provide an age pattern of mortality for paleodemographic populations, making them advantageous for analyses on mortality, morbidity, and fertility in archaeological populations where the sample sizes are too small to compute a normal life table based on the data alone. However, the primary danger is that a model life table is only as good as the model that is chosen. These tables impose a pattern of age-specific risk of mortality on the data without taking into consideration the observed mortality pattern. Thus,

the pattern imposed on the data may be inaccurate if the wrong model life table is chosen and lead to biased analyses (Gage 1988).

Age-Related Mortality at Petra

Newer methods for estimating age-at-death, such as cementochronology, have resulted in opportunities to circumvent many of the problems with traditional aging methods as well as the issues particular to the PNRP collection. For the PNRP population, establishing age-at-death in order to build paleodemographic models of mortality in Petra has been particularly difficult using standard aging techniques. Burial practices and postmortem disturbance in the form of bioturbation, looting, and flooding have caused many of the PNRP skeletons to be fragmented and commingled. Because of this, the skeletal elements necessary for age-at-death estimations, such as the pubic symphysis, are not always present or well-preserved. Commingling adds further difficulty for using multifactorial age estimation techniques, which are more accurate. Consequently, if a pubic symphysis and auricular surface of the pelvis are found separately, it is difficult to determine whether or not they belonged to the same individual. Cementochronology provides a more accurate age estimation technique in addition to circumventing many of the issues with preservation in the PNRP tombs because teeth are more likely to be preserved than the delicate bones of the pelvis.

With the age estimates, an age-at-death distribution and mortality profile can be established for the PNRP sample. Mortality models take on different shapes depending on the events that led to death (Gowland and Chamberlain 2005). For instance, attritional mortality models represent typical patterns of mortality where infants and young children experience high probabilities of mortality, which sharply drop during late childhood and again begin to gradually increase with age. Catastrophic models, on the other hand, are the outcome of events like disease epidemics or

natural disasters that indiscriminately kill by age. These resemble the demographic profile of living populations more so than attritional models, and are characterized by an unexpectedly high rate of adolescents and young-adults in the skeletal assemblage. By creating an age-at-death distribution, it is possible to determine whether the PNRP sample resembles an attritional or catastrophic model. This will help confirm whether or not the Petra North Ridge population did indeed experience a low prevalence of chronic physical stress as the paleopathological data indicates, or whether they may have succumbed to a virulent disease event with a high fatality rate.

Parametric hazard modeling allows for meaningful interpretations about mortality risk to be made with a small sample. Age-specific risk of mortality allows us to examine trends of mortality through time, at what rate they increased with age, and which age groups in a population were most vulnerable. By comparing the patterns of mortality risk to contemporaneous populations, the mortality data for Petra can be situated within its historical context to understand how the North Ridge population fared in comparison to their counterparts in other urban environments.

With these analyses, a mortality profile for the Petra North Ridge population can be generated. By doing so, we can begin to more confidently interpret previous research on the North Ridge population and create a framework in which to understand and interpret the results of future studies. Furthermore, by comparing the pattern of age-specific mortality risk at Petra to another large trade center connected to circum-Mediterranean exchange, Portus, we can also understand more fully how regional, local, and population level factors were embodied in this population in the form of mortality risk. As an archaeological population, this research contributes to our understanding of mortality risk in the past, how we can understand the trends of mortality risk

through time, and whether or not basic assumptions held about mortality rates in the past and in pre-industrial, urban populations can be substantiated or whether they should be reassessed.

Chapter 3: Materials and Methods

Sample Selection

The teeth selected for this study came from the 1999, 2012, 2014, and 2016 field seasons of the Petra North Ridge Project. In total, 315 teeth were determined to be suitable for cementochronology in terms of their preservation, which ranged greatly depending on the context. The vast majority of the teeth had very friable tooth roots and cementum that were prone to crumbling if not handled carefully. Of these teeth, the overwhelming majority came from commingled contexts. Only a very small sub-set originated from individual, primary interments in the tombs.

Complete teeth, identifiable tooth roots, and teeth still anchored in maxillae and mandibles that had all or a portion of the middle 1/3 of the tooth root necessary for cementochronology were selected. Tooth presence, metric and non-metric traits, and dental pathologies were recorded prior to destructive analysis using the forms and guidelines set by Buikstra and Ubelaker (1994). For the mandibles, if the mental eminence was present it was recorded and scored for sex estimations based on the same standards (Buikstra and Ubelaker 1994). However, this was only possible in a few cases and this sample size was too small to conduct any sex-based analyses. Photographs were taken of all teeth selected for this study to ensure that a complete record is available after they were processed for analysis.

Due to the commingled context of the samples, it was necessary to carefully identify teeth that could be soundly attributed to different individuals in order to prevent double-sampling. Contexts from within the tombs were differentiated and grouped together using stratigraphic and taphonomic evidence. The teeth belonging to each context were then examined based on tooth

type, side, position, morphology, and wear patterns. Establishing individuals was much more apparent for those still anchored in mandibles and maxillae. For these fragments, siding, overall morphology, and noting the presence and absence of key features, such as the mental eminence on the mandible and the nasal spine on the maxilla, were used to evaluate whether the mandibular and maxillary fragments belonged to different individuals.

When possible, at least two teeth were selected for each identifiable individual in order to increase the probability that a viable section of cementum would be collected and to help reduce intraobserver error when it came time to count the cementum annulations. Following the findings of (Charles et al. 1986; Wittwer-Backofen et al. 2004), incisors and first premolars were preferentially selected when possible. Third molars were completely omitted from selection due to the large standard deviation of the average age of tooth eruption. In the end, 34 incisors, 18 canines, 29 premolars, and 29 molars were used in this study.

The sample included teeth originating from 6 different tombs that had been excavated over the course of 4 field seasons (see Appendix A for a full list of the teeth). Of a total of 315 teeth, 110 teeth, representing 70 individuals, were chosen for the final sample (Table 3.1). Of

Table 3.1: Breakdown of the number of teeth used for cementochronology and the minimum number of individuals by tomb.

Tomb	Number of Teeth	Omitted Teeth	MNI represented by the sampled teeth
B.4	8	1	5
B.5	42	1	24
B.6	23		15
B.7	24	4	15
F.1	9	1	7
Tomb 2	4		4
Total:	**110**	**7**	**70**

these 110 teeth, 2 teeth were found to not have any viable cementum to count after sectioning. An additional 7 teeth were omitted after sectioning because it was determined that they were probably double sampled.

Sample Preparation

Before sectioning, the tooth roots were embedded in Caroplastic resin (Carolina Biological Supply, Burlington, NC) within either a 5 ml or 30 ml syringe, leaving the crown exposed for future research. The hardness of the resin was determined using the preparation guidelines for gross anatomy samples. Once the teeth were set in the resin, they were placed in a fumigation hood and left to sit overnight to allow the resin to harden. Once the resin set, the teeth were sectioned using a Buehler Isomet Low Speed Saw with a diamond wafering blade. Although 100 μm sections are ideal for this analysis, the fragility and friability of the teeth necessitated cutting sections of 400 μm thick, or even thicker (up to 900 μm) for some very fragile teeth.

After sectioning, the individual sections were wiped clean with an alcohol swab and placed in distilled water for 3-5 minutes in order to best ensure the removal of all debris left from the low-speed saw. The sections were then removed from the water, once again cleaned with an alcohol swab, and then mounted onto a glass slide using Crystal Bond™ as an adhesive. The sections were then sanded using increasingly fine gradients of sand paper until they were the appropriate thickness of 100 μm. The sections were first sanded with 180 grain sand paper until they were 200 μm and then 400 grain sandpaper until the sections measured 100 μm. At this point, 800 grain and 1200 grain sandpaper were used to smooth the surface and obliterate any lines left from sanding the process. Finally, the tooth was polished with Buehler Alpha Micropolish II with a particle size of 0.3 microns, wiped clean with an alcohol swab, and then wiped with a lens cloth to remove all remaining debris.

The number of slides for each tooth varied from 2 to 7 depending on the length of the tooth root. Due to time constraints, slides were processed until 3 good quality slides were obtained for each tooth. The remaining slides that were not processed were labeled and stored for future use if needed. The slides were viewed at 200X and 400X magnification with a Wolfe DigVu DVM 2.0 transmitted light microscope and multiple photographs taken for each slide. Due to the variable preservation of both the teeth and the cementum, the highest quality photo was identified for each slide and selected for counting. The photos were uploaded to Adobe Photoshop in order to increase the contrast between the dark and light bands of annulations to facilitate counting. The contrast was increased using the Auto Tone, Auto Contrast, Auto Color, Level Adjustment, and Unsharp Mask tools and then the text tool to mark and count the annulations (Figure 3). When all the slides had been processed, the annulation counts for each slide belonging to a single tooth were averaged together. The average age of tooth eruption, taken from the Atlas of Human Tooth Development and Eruption (AlQahtani et al. 2010), was then added to these figures. When there were multiple teeth representing the same individual, the age-at-death estimates for each tooth was averaged together to get the final age-at-death estimate.

Life-Table

These data were then used to generate a raw age-related mortality profile for the Petra population including calculations of the risk of mortality, *q*, in a particular age category, (q_x), and the average life expectancy, *e*, someone would expect to attain once reaching a particular age

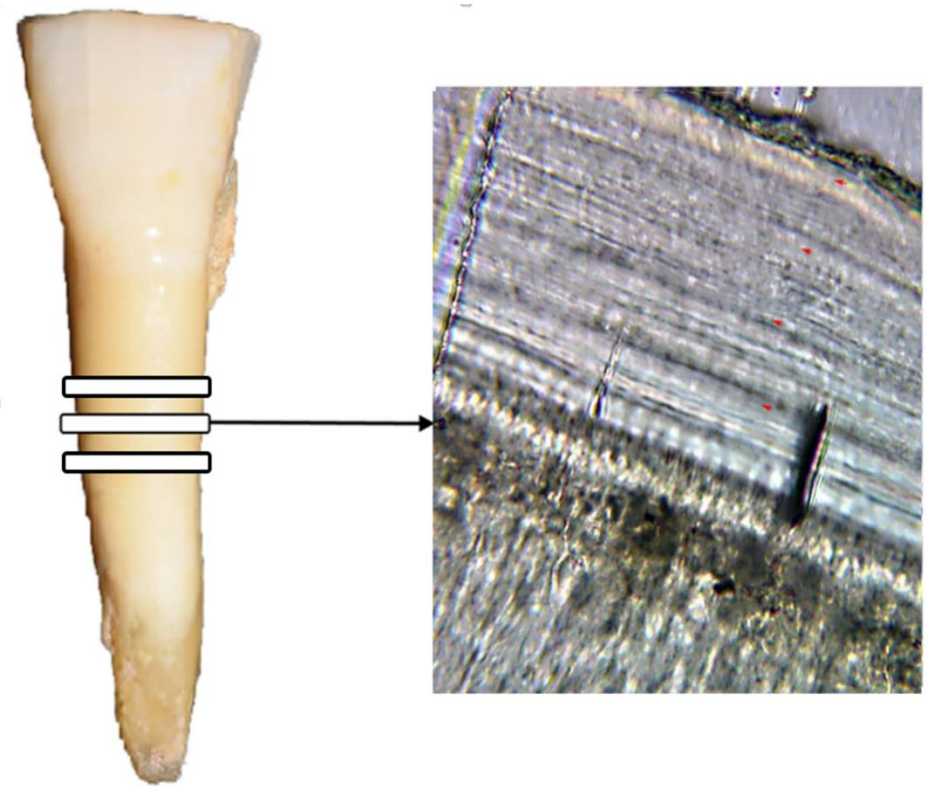

Figure 3: Section of cementum taken from a LI_2 (T141). The arrows mark every 10^{th} annulation.

category, (e_x). In this case, q_x is calculated as:

$$q_x = d_x / l_x$$

where l_x is the total population alive at the beginning of the age category x, and d_x is the number of individuals who die in age category x. In addition, life expectancy from a particular age category x is calculated as:

$$e_x = T_x / l_x$$

where T_x is the total number of person-years lived if an individual survived age category x and all subsequent age categories. These variables will allow assessment of the general effects of age on mortality at the site before application of a parametric hazard model.

Parametric Hazard Analysis

Parametric hazard analysis was used to establish age-specific risk of mortality based on the age-at-death estimates. Because no sub-adults were represented in the sample, a Gompertz-Makeham model was chosen to model adult mortality. The Gompertz-Makeham model includes two different components consisting of three parameters (Gage 1988; Wood et al. 1992, 2002). The Makeham component of the model consists of one parameter, α_1, which accounts for age-independent hazard of mortality that is constant throughout the human life-span. The Gompertz component consists of two parameters that account for the hazard of mortality due to senescence. The first parameter, α_2, models the risk of death due to senescence at birth. The second parameter, β, models the exponential increase of the hazard of mortality as an individual ages.

In order to estimate these three parameters, the program MLE was used (Holman 2005). MLE uses maximum likelihood estimates to find the parameter values of the Gompertz-Makeham model that maximize the likelihood of the age-at-death estimations given the parameters. The Gompertz-Makeham hazard function for mortality, shown below, was used to estimate the age-specific hazard of mortality (Wood et al. 2002: eq. 7.25). Once the age-specific risk of mortality was estimated, the values were graphed in Microsoft Excel.

$$\mu(a) = \alpha_1 + \alpha_2 e^{\beta\alpha}$$

MLE was also used to calculate differential rates of mortality between Petra and comparative populations. In order to identify any statistically significant differences in mortality risk between different sites and between tombs, the tomb number or the population was coded as

a discrete variable and modeled as a covariate acting upon the parameters of a Gompertz-Makeham model using the proportional hazard specification given below (DeWitte et al. 2013).

$$H(\alpha|x_i p)=h(\alpha)e^{x_i p}$$

In this program, the Gompertz-Makeham model is set as the baseline hazard, h(a), and the covariate, x_i, is the variable being tested (e.g., population). The variables were coded as either "0" or "1". Any negative estimate for the parameter suggests that the individuals from the skeletal sample coded as "1" had a decreased risk of death compared to the individuals in the tomb or skeletal sample coded as "0". A positive value then suggests that the individuals from the skeletal sample coded as "1" had an increased risk of death compared to those in the population coded as "0".

A likelihood ratio test (LRT) is used to assess the fit of the model given above and to determine whether or not the results are statistically significant. The formula for the likelihood ratio test is given below (DeWitte et al., 2013):

$$LRT = -2[\ln(L_{reduced}) - \ln(L_{full})]$$

The LRT approximates an X^2 distribution with df =1. This test assesses the fit of the full model compared to a reduced model where the covariate effect is set to 0. By doing so, the null hypothesis that the tomb an individual was interned in had no effect on mortality can be tested.

Analysis

In order to contextualize the results of the age-at-death distribution and the age-specific risk of mortality, they were compared to other sites in the circum-Mediterranean region (Figure 4). All of the comparative populations included sub-adults; however, due to the limitations of the Petra data only age estimates of 20 years or greater were used in the comparisons. The results from Petra were compared with Isola Sacra (n=88) was the necropolis for the inhabitants of the urban, port city *Portus Romae* in modern day Italy. The cemetery is located on an artificial island that extends 1.5 km along the road that connected the port city of Ostia and Portus. Similar to Petra, Portus was a major trading center for the Roman Empire. This cemetery was in use from the 1st - 3rd centuries AD but the sample used for age-at-death estimates date to the period of the cemetery's primary use in the 2nd – 3rd centuries AD (Geusa et al. 1999).

Figure 4: Map marking the location of Isola Sacra in relation to Petra, Jordan.

The age-at-death estimates for Isola Sacra were also derived from cementochronology (Geusa et al., 1999). When more than one tooth was sampled for and individual and there was thus more than one age estimate for an individual, the mean of the age-at-death estimates was calculated and used. The age-at-death distribution of Isola Sacra was compared to Petra's using a Kolmogorov-Smirnov 2-sample test to test for significant differences between the distributions of the data. In order to estimate age-specific risk of mortality for Isola Sacra, the Gompertz-Makeham parameters were also estimated using the program MLE (Holman 2005).

Together, these methods allow us to recover and analyze age-specific mortality risk in the North Ridge population. This method for age estimation establishes a more detailed age-at-death distribution for the Petra North Ridge population than those using standard morphological age estimation methods. Additionally, the hazard analysis allows us to estimate age-specific risk of mortality for a relatively small sample size without imposing its own pattern of mortality risk upon the data. Finally, comparing the age-specific mortality risks between Petra and Portus (Isola Sacra) allows us to better determine which factors may have had significant contributions to molding age-specific mortality risk in these populations and therefore highlight the aspects of the North Ridge populations' social and physical environment that affected them.

Chapter 4: Results

The mortality profile was generated with age-at-death estimates determined by adding together cementum annulation counts and the average age of tooth eruption (see Appendix A and B). Unlike other standard skeletal aging techniques, cementochronology provides point estimates of age-at-death. However, as is the case with any method, there is always a degree of standard error. Due to this, the age-at-death estimates were grouped into categories with 5-year increments (e.g., 20-24, 25-29…). Because no subadults were included in this analysis, the age-at-death distribution only includes adults over the age of 20 years.

At first glance, the distribution does not clearly conform to either a catastrophic or an attritional model of mortality (Figure 5). This may be a result of sampling bias, where there is an over or underrepresentation of individuals in certain age categories compared to the overall Petra population. In addition, it may ultimately be caused by "mimicry bias" (Bouquet-Appel and Masset 1982), where the age distribution of the original sample used by Al-Qhatani et al. (2010) to develop the dental eruption estimates influenced the age distribution of the age-at-death estimates for this sample. However, the age-range seen in samples used to develop dental age estimation techniques is relatively narrow and limited by the years during which children experience dental growth and development. Therefore, any potential bias would likely cause only a 1 to 2-year difference in the resulting age estimation.

Contrary to what might be expected, age-at-death distributions are very sensitive to changes in fertility, not mortality (Hoppa 2002). Due to this, the age-at-death distribution for a population is actually more demonstrative of trends in fertility. The spike in individuals in the30-39 age categories may therefore be indicative of population growth during this period. At the time that the cemetery sample was created there may have been more individuals aged 39 and

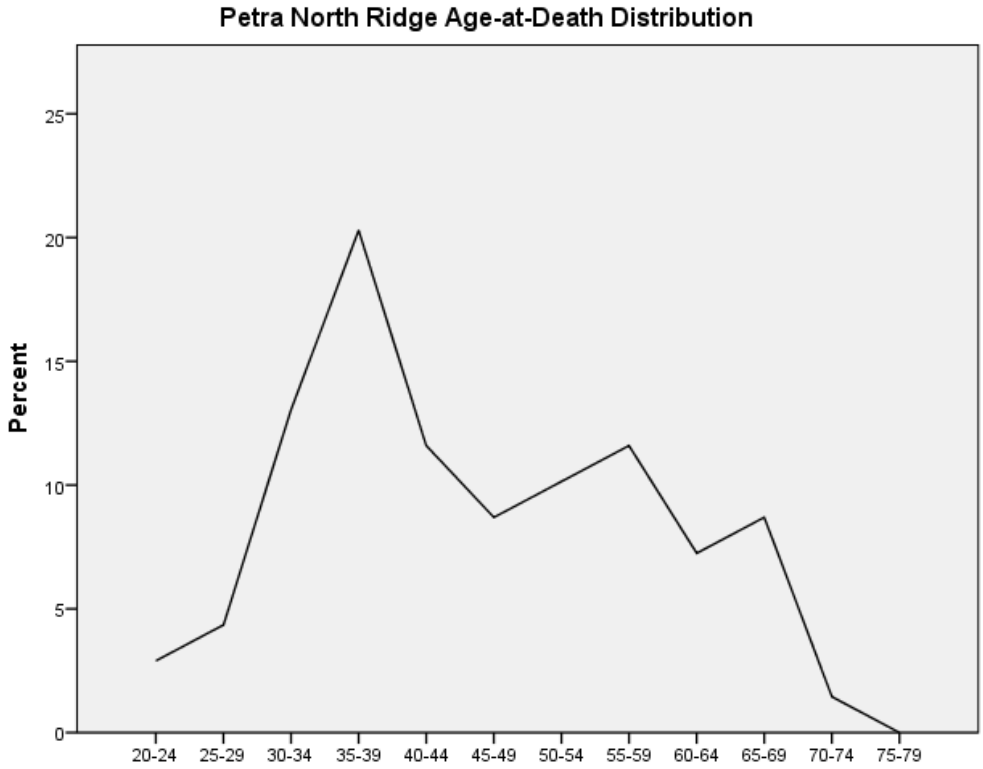

Figure 5: Age-at-death distribution for the Petra North Ridge population.

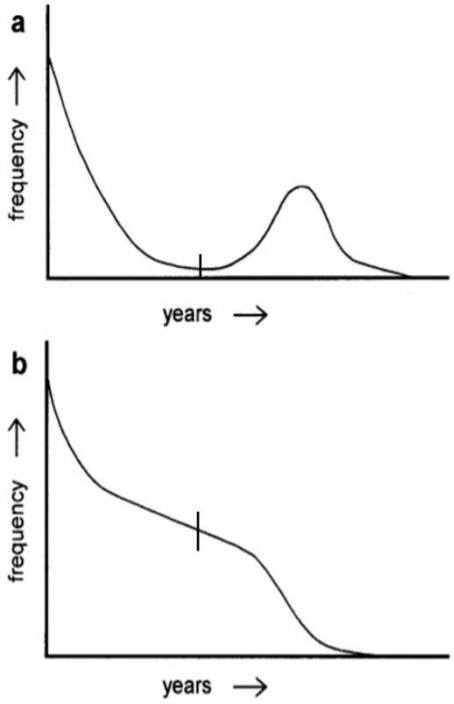

Figure 6: Example of an attritional model of mortality (graph a) and a catastrophic model (graph b; from Margerison and Knusel 2002). The vertical lines indicate the point at which the data for the North Ridge population begins.

under than there had been previously been due to population growth. This would result in a greater proportion of individuals in these age categories compared to the older age categories (i.e. 40 +). Additionally, the spike of individuals in these age categories may represent the migration of young adults into Petra from the surrounding regions. Migration into urban centers is a common phenomenon and young adults are one of the most likely age groups to migrate (Gage et al. 2012). The increase of individuals in these age categories may also be due in part to maternal mortality. The lack of individuals whose sex could be determined prevents any sex based analysis. Therefore, the abrupt increase of individuals aged 30-39 may not be anomalous, but a product of natural population trends occurring during this period.

The low percentage of individuals in the 20-24 age category compared the 45-49 and the 50-54 age categories would suggest a general pattern of attritional mortality where there is an increase in mortality risk in the older age categories. The decreasing representation of individuals in the oldest age categories (i.e. 55-59 through to 70-74) is also characteristic of attritional models of mortality. If it conformed to a catastrophic model there would be a greater percentage of individuals in the young adult age group (20-30 years old) and a steady decrease in the representation of individuals in the succeeding age categories (Figure 6). If the age categories above 50 are collapsed into a 50+ category, which is typical in archaeological samples due to the limitations of standard age-at-death methods, the shape of the data takes on a more apparent attritional shape (Figure 7). In this representation, the age-at-death distribution for the North Ridge population more clearly resembles the "bathtub" curve characteristic of attritional mortality models.

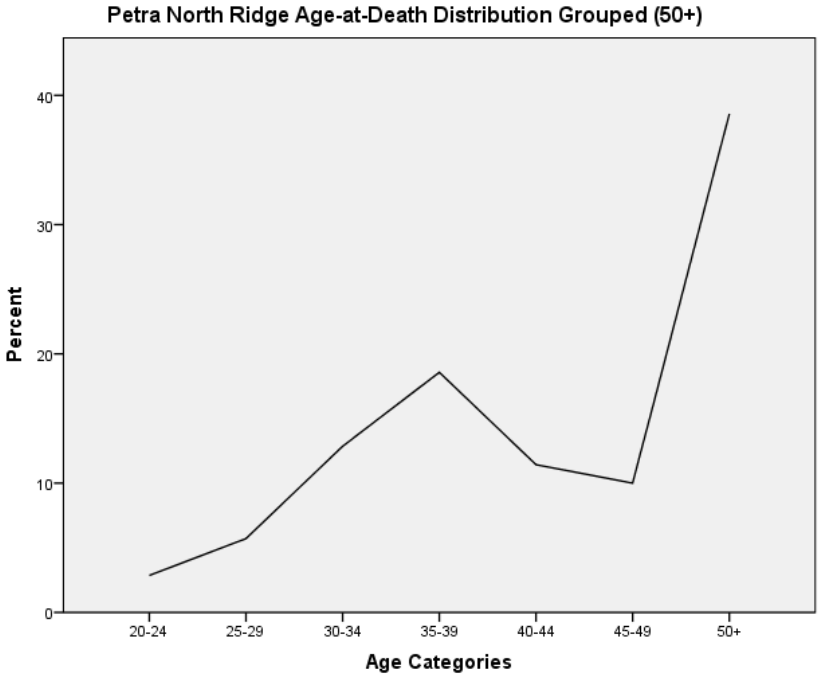

Figure 7: Age-at-death distribution for the North Ridge Population with the oldest age estimates grouped into a 50+ category.

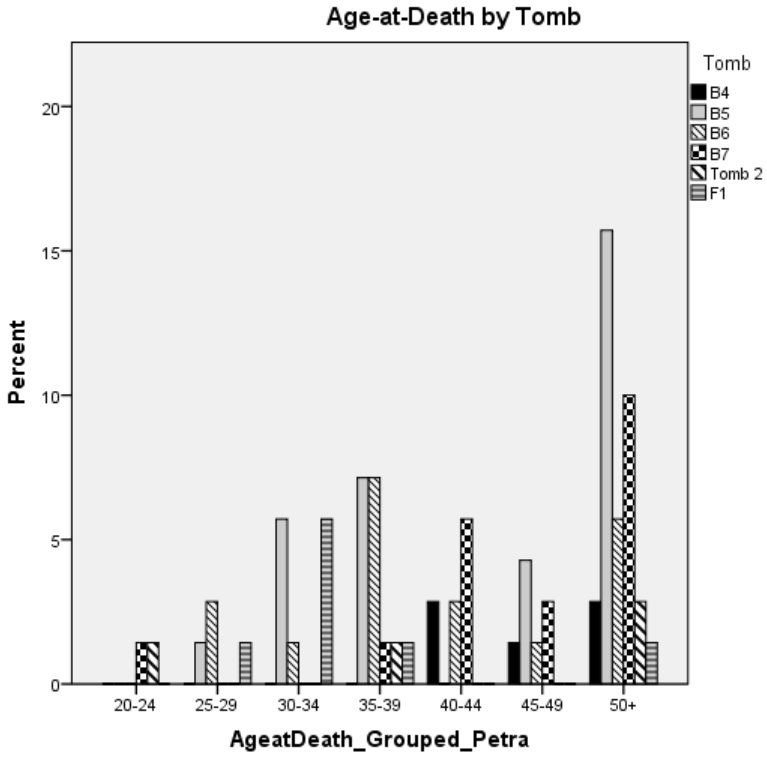

Figure 8: Age-at-death distribution broken down by tomb

The percentage of individuals in the older age categories is of particular interest. Approximately 40% of the sample falls into the age category 50 and higher. Of these individuals, approximately 12% are reaching the ages of 55-59, 10% the ages of 60-64, and 2% the ages of 70-74. This indicates that a large proportion of individuals are reaching relatively advanced ages. This corroborates well with the paleopathological data in which age related degenerative diseases are the most prevalent pathological conditions exhibited in the North Ridge population (Canipe 2014).

The age-at-death profile was further broken down by tomb to see if any one tomb could be pinpointed as the cause for the spike of individuals in the 30-39 age categories. Figure 8 indicates that tombs B5 and F1 are responsible for the spike of individuals in the 30-34 age category and tombs B5 and B6 for the spike in the 35-39 age category. The samples from tomb B5 and B6 largely originated from intact mandibles and maxillae that could easily be used to establish different individuals. Additionally, the estimates from tomb F1 originated from two intact skulls and premolars exclusively. Thus, it is unlikely that doubling was a significant factor in either of these cases. Tomb B5 had the most individuals in the 50+ category, suggesting that whatever the cause of the increase in individuals in the 35-39 age group, many were still living to older ages. Indeed, tombs B5 and B6 still appear to follow an attritional model of mortality where representation of individuals increases as age progresses.

The age-at-death distribution for the Petra North Ridge population was compared to that from Isola Sacra (Geusa et al. 1999), which showed a significant difference (Figure 9). The age at which mortality appears to peak for these populations differs considerably. Mortality peaks at the fairly young age of 25-29 for the Isola Sacra population compared to a peak at 50+ for Petra. This suggests that the individuals at Petra were living longer on average. Additionally, despite

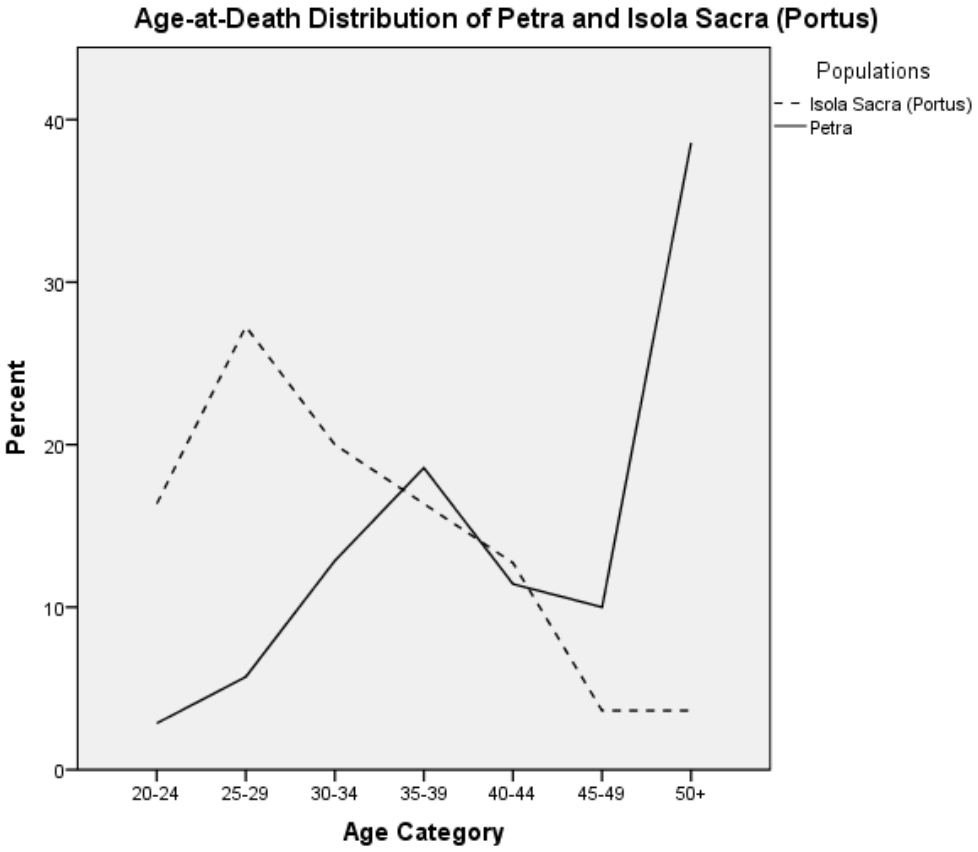

Figure 9: Comparison of the age-at-death distributions between Petra and Isola Sacra (Portus)

Table 4.1: Results of the Kolmogorov-Smirnov test between Petra and Isola Sacra.

Population	Kolmogorov-Smirnov Z-Value	Significance (2-Tailed)
Petra vs. Isola Sacra	2.342	.000

Petra and Isola Sacra both being urban centers as well as major trade depots for their respective regions, they all plot distinctly different age-at-death distributions, thus highlighting the variance in mortality that can occur between superficially similar populations.

Table 4.2: Gompertz-Makeham parameter estimates for the Petra North Ridge population and Isola Sacra.

Parameters	Petra	Isola Sacra
α_1	0.000000003047	0.019179036806
α_2	0.002720015668	0.003082207527
B	0.065051997231	0.085202874637

The age-at-death distributions from these sites were quantitatively compared using a Kolmogorov-Smirnov test. The results in Table 4.1 indicate that Petra and Isola Sacra had significantly different age-related mortality profiles at the 0.05 level. After determining that the North Ridge population follows an attritional model of mortality, the Gompertz-Makeham parameters were estimated using MLE to determine the age-specific hazard of mortality (Holman 2005). These are presented in Table 4.2 along with parameters from the comparative sample of Isola Sacra. A life table was also created based on the age-at-death estimates to generate the probability of dying in a particular age category in order to compare the results with those from the Gompertz-Makeham model.

As expected, the Gompertz-Makeham hazard model provides a smooth version of the one produced from the raw cementochronology age-at-death estimates (Figure 10). This is because the age-specific risk of mortality is not estimated based on the data itself, but rather the Gompertz-Makeham parameters. This is advantageous for small sample sizes like that for the North Ridge population for a number of reasons. In order to generate a life table, the larger data set needs to be broken down into age categories, thus dividing the data into much smaller sub-sets. Where the Gompertz-Makeham parameters are estimated based upon all 70 age estimates, the life table estimations divide these estimates into individual age categories containing as few

as one age estimate to calculate risk of mortality for each age interval. Furthermore, life tables require a parameter to be estimated for every age interval in the table. For the current data, that means that 11 parameters must be estimated as opposed to the three for the Gompertz-Makeham model. The more parameters there are in a model, the more data that are needed to properly estimate them. This makes life tables inapt for generating sound interpretations from small samples. Furthermore, parametric hazard modeling smooths out the data and corrects for small sample sizes. As such, parametric hazard modeling is a better way to generate age-specific risks

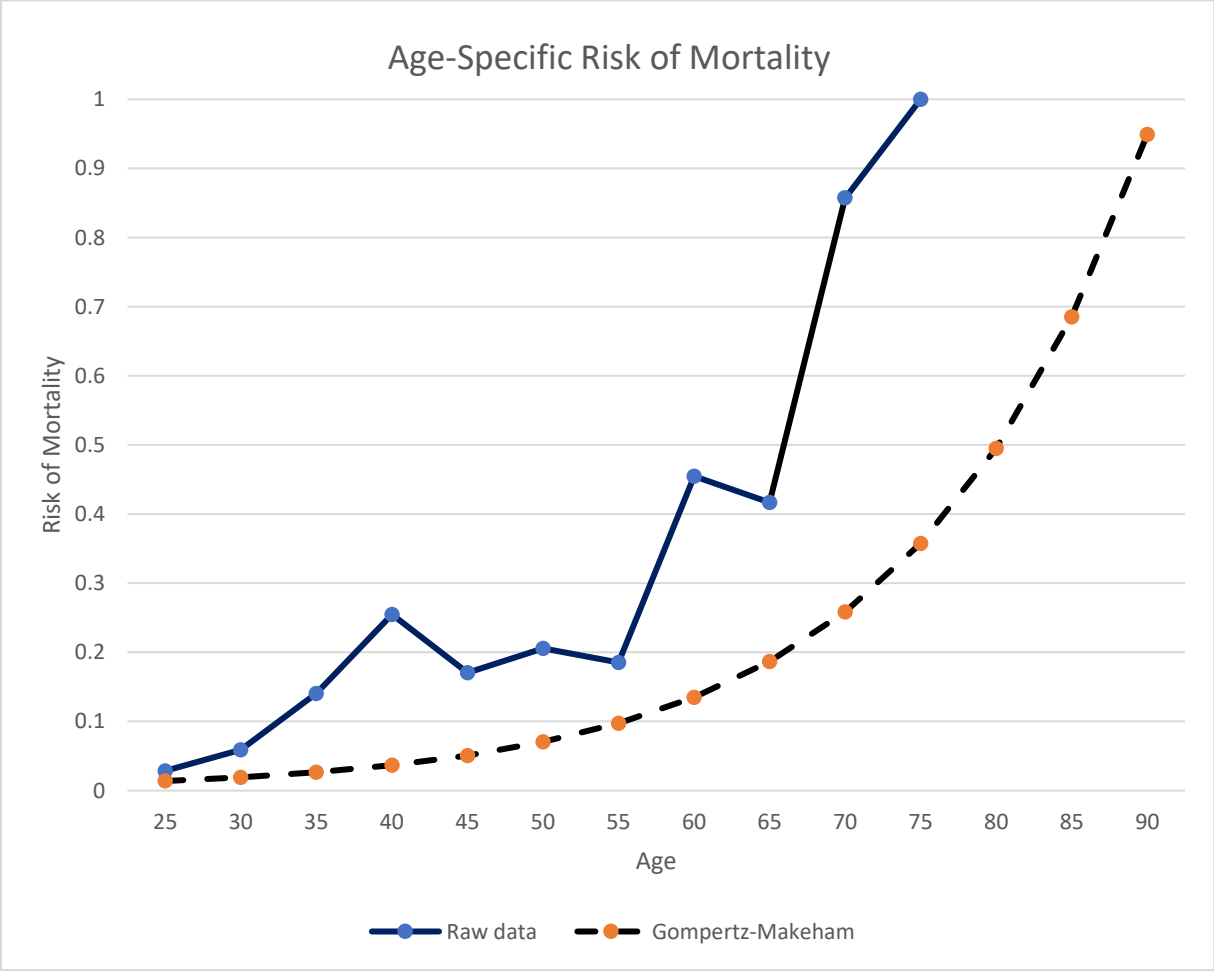

Figure 10: Comparison of the age-specific risk of mortality estimated based on the raw data and the Gompertz-Makeham model parameters.

of mortality that allow for meaningful interpretations with a small sample such as this one (Wood et al. 2002).

The sharp peaks in mortality at the ages of 35, 40, and 60 are smoothed out into a more gradual increase in mortality risk over time. Mortality begins to increase more significantly around the ages of 35 and 55 based upon the Gompertz-Makeham model, effectively mirroring the increases demonstrated in the raw data. However, the increases remain more gradual. In effect, the Gompertz-Makeham helped control for the potential biases or processes that resulted in a large proportion of individuals in the 30-39 age categories.

A consistent and significant difference between the mortality hazard calculated from the raw data and that from the Gompertz-Makeham model begins around the age of 70. This is due to the form of the Gompertz-Makeham model, which models a constant exponential increase of mortality risk with age. Due to this, the hazard of mortality in the oldest age categories (80 +) where a sharp increase in mortality risk might be expected effectively gets underestimated because the slope of the Gompertz-Makeham parameters is simply being projected forward. Caution must thus be used when interpreting mortality derived from the Gompertz-Makeham model for the oldest ages.

In order to determine whether Petra's age-specific mortality risks are relatively low or high, mortality risk was compared between Petra and Isola Sacra. The age-specific risk of mortality for Isola Sacra was also calculated using the Gompertz-Makeham model and the parameters estimated with MLE (Geusa et al. 1999; Holman 2005).

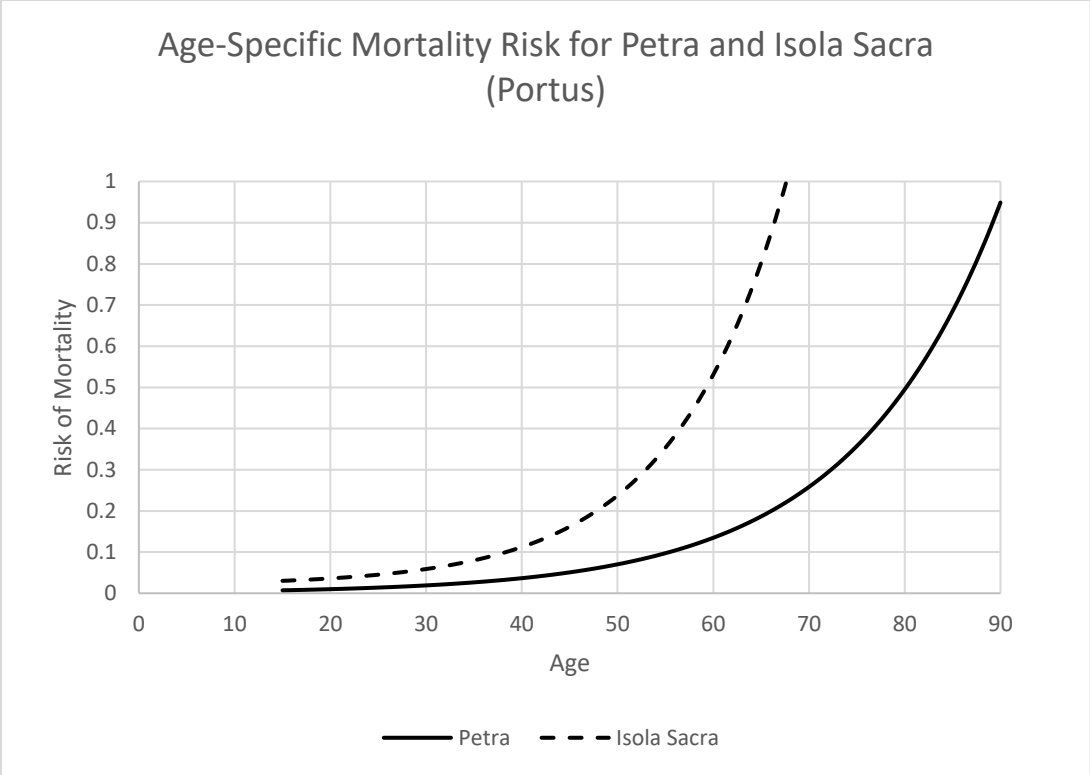

Figure 11: Comparison of the age-specific risk of mortality between the Petra North Ridge Population and Isola Sacra.

Compared to Isola Sacra, Petra has a lower risk of death across all age categories (Figure 11). The risk of mortality particularly begins to diverge during middle adulthood around which time Petra begins to plot a significantly lesser mortality risk. When the parameters are compared to one another it is evident that although Isola Sacra had a lower risk of mortality due to senescence at birth, however, the age-independent risk of mortality and the rate at which mortality risk increases over time is markedly greater than Petra's.

A differential mortality analysis was run to discern whether or not there are any significant differences in mortality risk between these two populations. Due to the small sample size of the individual tomb populations, the same test could not be run to determine whether or not there were any significant differences between the tomb samples. The results of the analysis confirm that

Table 4.3: Results from the differential mortality analysis.

Population	ha_population	Standard Error	P-Value
Petra vs. Isola Sacra	1.22	0.18	0.00

there was indeed a significant difference at the 0.05 level (Table 4.3). The ha_population value of 1.22 indicates that the inhabitants of Isola Sacra experienced a significantly greater risk of mortality compared to their counterparts in Petra. The mortality patterns for Isola Sacra conform to expectation of high mortality risk for a pre-industrial, urban population. The difference between these two suggest the North Ridge population experienced lower risks of mortality than other contemporaneous urban populations in the broader Mediterranean region.

Together, these data suggest that the Petra North Ridge population's age distribution does indeed conform to an attritional model of mortality and that Petra experienced relatively low rates of mortality risk compared to the Roman site of Portus/Isola Sacra. Isola Sacra did indeed significantly differ from Petra which suggests that environmental and socio-cultural differences on the regional and population level resulted in significantly different risks of mortality despite their shared urbanity and roles as economic depots.

Chapter 5: Discussion

The difference in age-specific mortality risk between the North Ridge population and Portus highlights how this segment of Petra's population diverges from traditional expectations concerning mortality in pre-industrial, urban populations. By comparing this portion of Petra's population to that from Portus we might begin to better understand how different aspects of their environmental contexts impact age-specific mortality. Despite their geographic distance, these two urban sites share many qualities inherent to ancient cities, such as high population density and mobility. However, key differences between these two populations may highlight the mechanisms and processes that underlie the differences in age-specific mortality.

Understanding the various processes and factors that contribute to a population's mortality risk is difficult. Understanding mortality involves breaking down multi-faceted, interconnected, and complicated variables and processes that are contextually dependent. For archaeological populations, understanding these variables and how they affected a population's mortality risk is limited by what can be discerned from historical and archaeological sources. The assessment of other variables from Portus and Petra reflecting morbidity and mortality, such as dietary composition and disease- and injury-related skeletal lesions, will illuminate the patterns seen in the age-specific mortality at each site. These results will then be assessed within the disease ecology of Petra and Portus, including the sites' political, economic, ecological, and demographic environments, to best understand the differences seen in hazard of death by age at the two sites.

Dietary composition:

Individuals with a nutritionally adequate diet consisting of sufficient and balanced levels of carbohydrates, fats, and proteins tend to have decreased risks of mortality (Bazelmans et al.

2006; Floud et al. 1990; Fogel 2004; Gage and O'Connor 2009; Sommer and Loewenstein 1975). For instance, Gage and O'Conner (2009) found that populations with diets high in carbohydrates and low in fats had a higher rate in senescent mortality with age than low carb and high fat diets. Moreover, the synergistic relationship between malnutrition and infectious disease means that the presence of one variable increases the susceptibility to the other (Chen et al. 1981; Scrimshaw 2000). Thus, an individual's and population's diet can be directly related to mortality.

The archaeological and isotopic data on dietary composition from the Near East demonstrates relative homogeneity from the Neolithic to the Byzantine Period (~7,500 BC – AD 640) (Al-Bashaireh and Al-Muheisen 2011; Al-Shorman 2004; Aufterheide et al. 2003; King 2001; Losch et al. 2014; Sandias 2011; Touzeau et al. 2014; White and Armelagos 1997; White et al. 1999) with the North Ridge population falling into this profile (Appleton 2015). The average carbon isotope values from bone collagen at Petra ($\delta^{13}C$ $\bar{x}$=18.3 ±0.3‰) is essentially the same as faunal bones tested from the site ($\delta^{13}C$ $\bar{x}$=18.5 ±0.6‰), while the average human nitrogen isotope value ($\delta^{15}N$ $\bar{x}$=9.5 ±1.6‰) is enriched by 1‰ over fauna ($\delta^{15}N$ $\bar{x}$=8.4 ±0.8‰) (Appleton 2015). This pattern implies that a significant portion of C_3 plants comes from the direct consumption of grains in addition to C_3-consuming sheep or goats (or their byproducts) (DeNiro and Epstein 1981). Appleton (2015:59) notes that these stable isotopic values of carbon and nitrogen in human bones from the North Ridge correspond with zooarchaeological and paleobotanical data at Petra that includes mostly C_3 plants such as wheat, barley, legumes, nuts, fruits and vegetables along with a many protein sources such as pigs, chickens, fish, and goats along with their secondary products.

The stable isotopic data for Isola Sacra indicate this population's diet differed slightly from the North Ridge, particularly in terms of the source and amount of protein in the diet. The high nitrogen levels at Isola Sacra ($\delta^{15}N$ $\bar{x}$=10.8 ±1.2‰) suggest that marine resources formed an

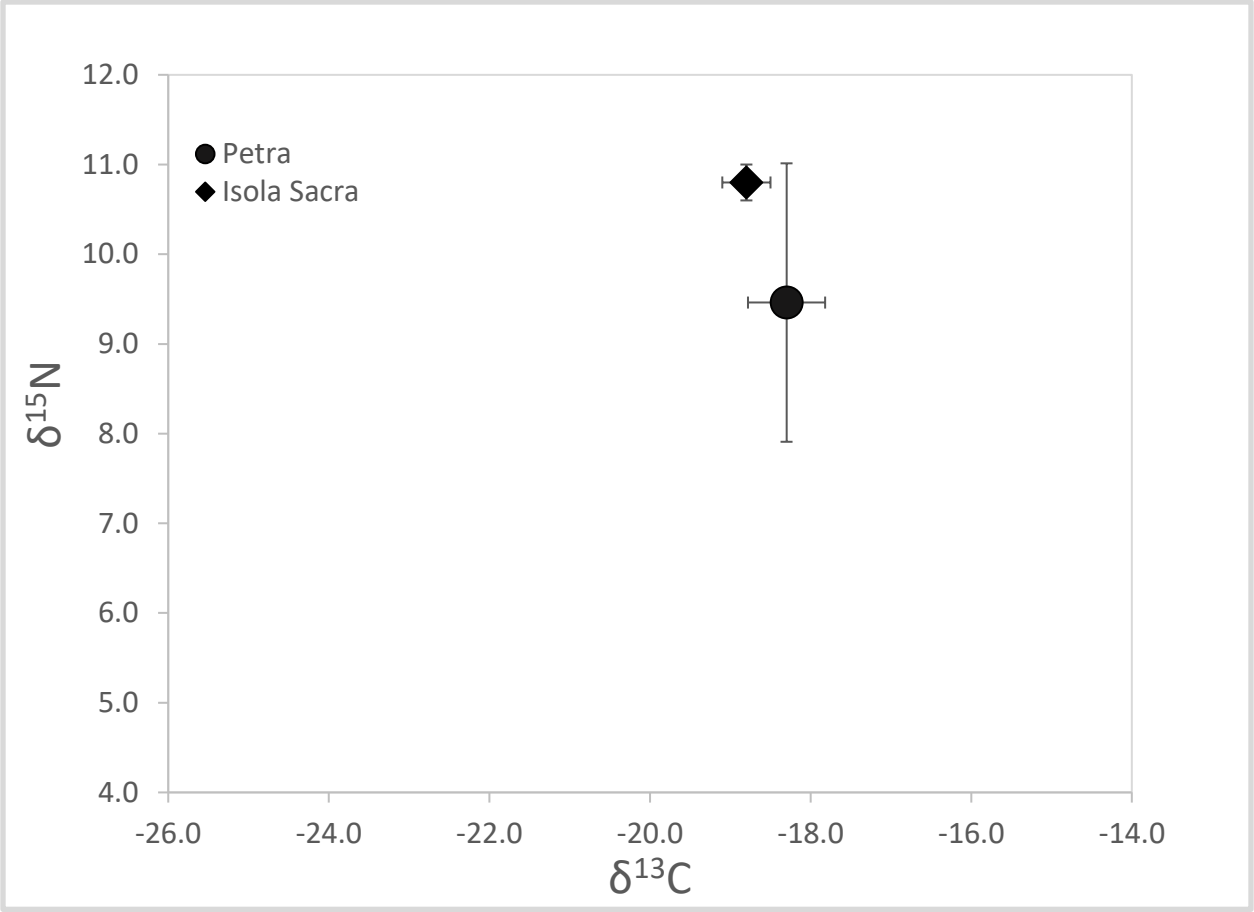

Figure 12: Stable carbon and nitrogen isotopic values of bone collagen at Petra and Isola Sacra with 1σ standard error.

important part of this population's diet, estimated at 40%, although the trophic level of the marine sources consumed varied between these individuals (Prowse et al. 2004). In addition, carbon isotope values from collagen ($\delta^{13}C$ $\bar{x}$=18.8 ±0.3) assert that a large portion of the diet, estimated at 60%, was based upon C_3 plants, such as wheat, and the animals who fed on them (Prowse et al. 2004). The elaborate 'Tomb of the Harvester' at Isola Sacra supports the importance of grain to this population (Prowse 2001), not only in terms of consumption but also as a significant import through the port. Other scholars have suspected that meat-based protein probably was available

only to the wealthier segments of those on the Italian peninsula, since the physical geography around Rome was not conducive to large-scale animal husbandry (Garnsey 1999).

Neither Isola Sacra nor Petra follow the pattern expected in a population receiving most of its dietary protein from animals or their byproducts (DeNiro and Epstein 1981). Petra's slightly enriched $\delta^{13}C$ values compared with Isola Sacra may indicate higher consumption of C_4 foods (or C_4-consuming animals) at the site. However, the fauna at Petra, which would be predicted to be eating lower-quality C_4 grains such as millet generally not favored by humans, have an even lower $\delta^{13}C$ value than humans, a pattern following that of Isola Sacra. Prowse and colleagues (2004) attribute this enrichment of human carbon values to the consumption of marine resources at Isola Sacra. This is not out of the question at Petra, as the remains of fish and containers for the fish-sauce *garum* have been recovered at the site. In addition, it is unlikely that humans at Petra subsisted on C_4 plants while the animals they ate grazed on the remnants of C_3 grains. Petra's lower $\delta^{15}N$ value than Isola Sacra reflects the lower level of marine consumption at the site, but may also suggest they consumed more nitrogen-fixed plants such as legumes than Isola Sacra (DeNiro and Epstein 1981).

Thus, in general both Petra and Isola Sacra had diets with a substantial protein component, mostly terrestrial in the case of Petra, but a notable marine component at Isola Sacra. C3 plants comprised the majority of both diets, which not only could include grains such as wheat and barley but fruits and legumes. Thus, it appears the similar diets at the sites may not be a sound explanation for differences in age-related mortality patterns.

Physiological Stress:

Physiological stress can result from a number of conditions, both psychological and physical, that cause disruptions or impairments to the body and may manifest in the skeleton and thus be observed through paleopathological analysis (Ortner 2003). This stress can in turn result in increased frailty, or increased susceptibility to mortality (DeWitte and Wood 2008; Jowett 1991; Zuckerman, 2012; Yaussy et al. 2016).

Two non-specific indicators of stress and two indicators of metabolic deficiencies were observed in the Isola Sacra and Petra North Ridge skeletal samples: porotic hyperostosis/cribra orbitalia, dental enamel hypoplasias, and evidence for Vitamin C and Vitamin D deficiencies. Porotic hyperostosis and cribra orbitalia result from the expansion of the inner trabecular bone, or diploe, of the cranium resulting in the destruction of the outer compact bone and a sieve-like appearance on the cranial vault (porotic hyperostosis) or the inside of the eye orbits (cribra orbitalia) (Ortner 2003; Walker et al. 2009). It is generally understood that porotic hyperostosis and cribra orbitalia can result from congenital anemias such as thalassemia, other hemoglobin abnormalities, or acquired anemia due to an individual's diet or from parasitic infection (Walker et al. 2009). Because this condition has multiple etiologies, it is considered a non-specific indicator of physical stress. Dental enamel hypoplasias (DEH) is characterized by transverse lines or pits observable on a tooth's enamel and is the result of the disruption in enamel formation during childhood (Goodman et al. 1980). DEH can result from a multitude of physical and psychological stressors and is thus considered to be a non-specific indicator of childhood stress.

Metabolic deficiencies, on the other hand, result directly from ailments such as Vitamin C and Vitamin D deficiency which can subsequently result in conditions, such as scurvy and rickets/osteomalacia respectively, that can affect the skeletal system (Brickley and Ives 2008). IN

particular, sustained Vitamin C deficiency inhibits the body's ability to sustain bone matrix formation and can thus manifest skeletally in the form of increased porosity and/or the presence of periosteal lesions throughout the skeletal system, but most notable on the skull and long bones (Brickley and Ives 2008). Vitamin D is a crucial element for the absorption of calcium and phosphorus, essential components of bone mineral. Vitamin D deficiency thus inhibits bone mineralization and the resulting decrease in bone density and strength can lead to mechanical deformations, such as bowing of the arms and legs, and altered growth of bones characteristic (Brickley and Ives 2008).

As can be seen in Table 5.1, the frequency of anemia-related lesions, cribra orbitalia and porotic hyperostosis, show no significant difference between the two sites. Petra has no cases, and only 1.6% of the individuals studied by Cho (2002) had signs of these lesions, suggesting that acquired anemia, such as iron or protein deficiencies, excessive parasitic infections, renal failure, or congenital anemia causing diploic expansion were not endemic in these populations. Additionally, there were no observed causes of scurvy or rickets reported for the North Ridge population and the Isola Sacra sample, suggesting that vitamin c and d deficiency was not prevalent among the North Ridge and the subset of 124 individuals examined by Cho (2002). Recent evaluations of the Isola Sacra sample have, however, revealed a notable presence of Vitamin D deficiency within this population (Prowse personal communication). More information on the presence of vitamin D in Isola Sacra is forthcoming, however, its presence suggests that Portus' population did indeed suffer from megaloblastic conditions and thus experienced more nutritional stress than the North Ridge population. Additionally, significantly more children at Isola Sacra suffered from physiological stress resulting in enamel formation disruption than at

Table 5.1: Frequencies of skeletal lesions observed at Petra and Isola Sacra

Site	Porotic hyperostosis/ cribra orbitalia		Dental enamel hypoplasia	
	n	%	n	%
Petra[a]	670	0	28	18
Isola Sacra	124	1.6[b]	58	81[c]

[a]Canipe 2014 – Porotic hyperostosis and criba orbitalia reported as a frequency of observable parietals, frontals, and occipital fragments; dental enamel hypoplasias, scurvy, and rickets are reported by the MNI of the sample
[c]Manzi et al. 1999 – Dental enamel hypoplasia reported by number of individuals

Table 5.2: Results of Fisher's Exact Test

Results of Fisher's Exact Test (p-value)	
Porotic Hyperostosis/ Cribra Orbitalia	0.0242
Dental Enamel Hypoplasia	0.000

Petra. This suggest that Portus' inhabitants were suffering a far greater prevalence of non-specific stress during their childhood.

Fisher's exact tests were run to test the significance of the differing prevalence of porotic hyperostosis/ cribra orbitalia and DEH between Petra and Portus. The results indicate that the differing prevalence of these paleopathological conditions are significant at the 0.05 level. This suggests that Portus' population was experiencing a significantly greater prevalence of these conditions and thus greater degrees of non-specific physical stress than the North Ridge population. This could have subsequently resulted in the higher rates of mortality risk observed for this population.

These data could indicate that physiological stress in the form of infectious disease or malnutrition did not significantly contribute to mortality risk in the Petra North Ridge population.

Conversely, the relatively low frequency of these conditions could also result from the North Ridge sample having a higher level of frailty than Portus. For instance, they could have succumbed to physiological stress due to disease or malnutrition before any skeletal indicator could form (Wood 1992). However, if this was indeed the case, the North Ridge cemetery sample would be expected to show higher age-specific mortality risk compared to Isola Sacra. The mortality hazard models instead suggest that the individuals in the North Ridge sample did not succumb to virulent diseases with high fatality rates, such as crowd diseases, and were generally living longer than their counterparts in Portus. Thus, the low levels of pathological indicators discussed above support a Petra population with greater longevity than at Portus.

The differing prevalence's of paleopathological conditions, such as dental enamel hypoplasia in particular, mirrors the significantly greater degree of age-specific mortality risk demonstrated in Portus's population when compared to Petra and may begin to explain the different patterns of age-specific mortality between the two populations. However, the prevalence of paleopathological conditions in a population is often the result of other environmental variables, such as a population's social and physical environment, and thus does not completely explain the underlying cause in the differing mortality risks.

Political-Economic Environment:

Adopting a political economic approach can highlight how global and regional systems at the macro-level can have acute consequences on the community- or site-specific micro-level (Goodman and Leatherman 1998). Previous studies have outlined the explicit connections between broader political and economic environments and specific populations in both the past and present (Bengtsson 1999, 2004; Croke 2012; Crooks 1998; Daltabuit and Leatherman, 1998; Defo 2014; DeWalt 1998; Goodman 1998; Leatherman 1998, 2005; Santos and Coimbra 1998; Swedland and

Ball 1998). In this case, the larger political and economic climates of Petra and Portus may explain their diverse age-related mortality and paleopathology profiles.

The 1st century BC to the 1st century AD was a period of vast physical and political development in Petra and the Nabataean Kingdom. By the 1st century BC, a formal monarchy, a permanent standing army, temple-based financial institutions, and a vast water-supply network had emerged (Johnson 1987; Negev 1977b; Schmid 2002). At the same time, the Roman Empire was increasing its presence and involvement in the eastern sector of the Mediterranean (Bowersock 2003; Schmid 2002). By the beginning of the 1st century AD, Rome had created the province of Judaea and was officially at the borders of Nabataea (Millar 1993). Rome and its client kingdoms intermittently invaded Nabatean territory during the 1st century BC into the 1st century AD (Millar 1993), but these various military assaults did not seem to hinder the movement of luxury goods such as spices and perfumes into the circum-Mediterranean region.

The 1st century AD Roman Empire was similarly characterized by political and economic stability (Prowse 2001). The Roman Empire experienced the expansion of agricultural production, increased urbanization, and the wider distribution of trade goods during this period (Prowse 2001). In fact, the increased surplus in the Roman Empire stimulated a growing demand for luxury items, which subsequently promoted trade and production in Nabataea and Petra (Fiema 2003; Johnson 1987). The Nabataeans capitalized on their increased trade connections by not only continuing the trade in raw materials, such as frankincense and other aromatics, but also the trade in luxury items they began manufacturing from these materials, such as perfumed oils (Fiema 2003; Johnson 1987). The Nabataeans' the dynamic trade role may have led to prosperous economic conditions in conjunction with a potentially stable political environment, which together may have contributed to lesser mortality risk in Petra through factors such as resource availability and

favorable market prices. Unfortunately archaeological or textual data have not enlightened much regarding Nabataean internal politics exists to support this hypothesis. The lack of skeletal lesions related to infectious diseases or malnutrition (Canipe 2014) and isotopic evidence for notable meat protein in their diet (Appleton 2015) would support an idea of prosperity and stability, as discussed below.

Portus also served an important role as a trade *entrepôt* due to its location on the Mediterranean cost ca. 23 km from Rome. The port was first established in the 1st century AD after the old port of Ostia became unusable due to the progressive silting up of the waterway (Meiggs 1973; Prowse 2001). By the 2nd century AD, Portus was handling most commercial traffic headed to Rome (Prowse 2001). A cemetery containing some of the inhabitants of Portus during the 2nd to 3rd centuries AD has helped illuminate the lives of some port city residents. Epigraphic evidence indicates that those buried at Isola Sacra were primarily middle and lower-class citizens, freedmen, and slaves who were administrators, traders, and merchants and whose livelihood was thus directly tied to the ports (Germani et al. 2011; Mannucci and Verduchi 1996; Manzi et al. 1991; Meiggs 1973; Pavolini 1986; Baldasarre 1990). The well-being of this population thus was intimately linked with Rome's involvement in the trade economy.

Unlike the economic prosperity of Petra in the 1st century AD, 2nd – 3rd century AD Portus was characterized by a transition to growing uncertainty. Portus during the 1st century AD until the end of the 2nd century was situated a hub for overseas trade, and its inhabitants were positioned to directly benefit from the thriving economic conditions. The end of the 2nd century until the 4th century however was characterized by political instability and civil war, which had wide-ranging effects on local governments throughout the empire (Meiggs 1973; Prowse 2001). The breakdown of centralized power caused major industries, such as the brick industry in Ostia, to collapse

(Meiggs 1973). The import of goods also decreased significantly – for instance, the decline in imperial building projects due to the rapid turnover of emperors reduced the importation of marble (Meiggs 1973). The well-being of Portus' inhabitants, whose livelihoods were connected to the ports, probably became increasingly uncertain, and in fact isotopic analysis of the Isla Sacra skeletons has found that this instability impacted accessibility to food (Prowse 2001), as discussed below.

Therefore, as the North Ridge population navigated a period understood to be the Nabataean Kingdom's political and economic zenith, Portus' inhabitants faced different realities. Those who lived and died during the 2nd century AD probably experienced relative political and economic stability. Much like Petra in the 1st century BC to the 1st century AD, Portus was flourishing during the 2nd century as the maritime entry way to Rome. With the breakdown of imperial governance, however, political and economic instability spread throughout the empire from the end of the 2nd century AD throughout the 3rd century AD. Portus' population, whose livelihoods and well-being were directly linked to the economic prosperity of Rome and the empire, were likely affected by the consequences of this instability. This instability may have in turn led to increased risk of mortality for those buried at Isola Sacra when compared to the North Ridge population.

Urban Environment:

The inhabitants of Petra and Portus were both managing life in urban environments which would have played an important role in shaping these populations' mortality risk. The increased population density (Barrett et al. 1998; Cockburn 1971; Morse 1995; Zuckerman 2014), associated build-up of human waste (Cohen 1989), attraction of insect and rodent vectors (Cohen 1989; Morse 1995), and the mobility of urban populations (Farmer 1996; Mayer 2000; McNeill 1976; Morse

1995) are often associated with increased disease-related mortality risk for urban populations compared to their rural counterparts.

Furthermore, urban-level population density can allow for the ongoing transmission of the more virulent but short-lived crowd diseases, such as smallpox, measles, and pertussis (Zuckerman 2014). Crowd diseases have been significant contributors to disease-related mortality throughout history (Bartlett et al. 1998; Zuckerman 2014). However, they are difficult to maintain in non-urban populations because they confer immunity on survivors, resulting in a reduced pool of potential hosts over time (Ornstein and Gay 2004). Measles, for example, has an endemic threshold of 250,000 to 500,000 (Bartlett 1957; Black 1966).

The estimated populations of Petra and Portus fall far below this threshold. Petra's population has been tentatively estimated at 30,000 (Joukowsky 2001). There is no known population estimate specifically for Portus, however Portus and Ostia are often discussed in tandem with one another and Ostia is often used to extrapolate information about Portus. Ostia became a large urban center with an estimated population of around 21,874 (Storey 1997) due to its economic importance (Meiggs 1973). As Portus had eclipsed Ostia in commercial and economic significance by the 2nd century AD, it might be inferred that Portus' population size was similar to that of Ostia by this period. Based on this, if any crowd disease did develop and was introduced to Petra or Portus, it could not have become endemic. However, both cities could have experienced repeated epidemics through the introduction of susceptible hosts through the reproduction and immigration of previously-unexposed individuals over time (e.g., Ornstein and Gay 2004). Population mobility could have increased the risk of new or repeated infectious diseases in both cities and subsequently increase mortality risk (Farmer 1996; Mayer 2000; Morse 1995).

Petra and Portus' roles as economic centers meant they both contained very mobile populations. For instance, Strabo refers to Petra having a thriving and diverse foreign population (*Geog.* 16.4.21-26). Petra's role as an economic center during the 1st century BC to the 1st century AD would have also resulted in less permanent migrants from the Red Sea, the Arabian Peninsula, and the circum-Mediterranean region coming to and from the city for trade. Additionally, the spike of individuals in the 30-39 age categories in the age-at-death profile may reflect in-migration to Petra from the surrounding areas. The analysis of strontium and oxygen isotopes on a subset of 61 individuals from the Isola Sacra sample revealed that approximately 1/3 of these individuals were born outside the region of Rome (Prowse et al. 2007). Isotopic data collected on third molars further indicated that these individuals migrated as children, presumably with their families (Prowse et al. 2007). Prowse and colleagues (2007) suggest that this migration would have been critical for maintaining Portus' population among conditions of high mortality. Like Petra, as the commercial portal to Rome, there is no doubt that less permanent migrants in the forms of merchants and traders regularly traveled to and from Portus from all over the Mediterranean. Thus, new diseases could have been easily and regularly introduced to both of these populations due to population mobility.

Differences in residential infrastructure may shed some light on the variation in the prevalence of paleopathological conditions and age-related mortality risk patterns between Portus and Petra. Domestic occupation at Portus likely included *insulae*, three to six-storied apartment buildings which outnumbered individual houses in Rome and Ostia (Meiggs 1973; Storey 2001, 2002). These residential buildings would have resulted in much higher population density than in Petra, which contained one-to-two story attached housing complexes (Kolb 2002; Parker and Perry 2014). This could have in turn resulted in increased probabilities of the contraction and spread of

infectious diseases throughout Portus' population and promoted higher rates of non-specific stress seen in the paleopathological data and thus resulted in increased disease-related mortality.

Petra's clean water has also been cited as a possible factor responsible for the low prevalence of paleopathological conditions within the North Ridge population and may have similarly played a role in the low levels of age-related mortality risk (Canipe 2014). The water supply for Petra and Portus, however, were quite similar to one another. Both had water supplies that originated from spring fed sources (Ortloff 2005; Petriaggi et al. 1995). Water was carried into Petra primarily through clay pipes (Oleson 2007; Ortloff 2005) and into Portus via a cement-lined aqueduct (Meiggs 1973). In both cities, these water sources were supplemented by covered wells and covered cisterns that collected rainwater run-off (Oleson 2007; Ortloff 2005; Meiggs 1973). Therefore, Petra's water system does not seem a likely contributor to the differing rates of mortality risk between these populations.

Regional Demography:

The differences in mortality, especially disease-related mortality, between Petra and Portus could also be caused by the larger, regional environments within which they were situated. The city of Portus, located in the heart of Rome, was located within a short distance from multiple large, densely settled urban settlements where infectious diseases were more likely to be contracted (Figure 13). Rome, in particular, is known for having an immense population for a pre-industrial city. Scholars had suggested that the city had a population of 1 million (Bairoch 1989; Brunt 1971; Hodges and Whitehouse 1983; Robinson 1992; Stambaugh 1988), however, reevaluations of the geography of Rome and urban densities in other cities such as Ostia and Pompeii have generated revised population estimates to around half a million (Storey 1997).

As all overseas commercial activity headed for Rome went through Portus, these two populations were intimately linked economically and physically. Portus was also connected directly to Ostia, with an estimated population of 21,874 (Storey 1997), by the Via Flavia (Meiggs 1973). Portus was thus immediately linked to multiple large, urban environments which could have easily promoted the contraction and transmission of infectious diseases within and between these populations through population mobility and commercial activity. In contrast, Petra was not so directly surrounded by urban settlements of equal size to Ostia or Rome. The broader regional landscape that Petra was situated in might be characterized as being less densely settled and less populated than that surrounding Portus. More systematic surveys of both regions could illuminate

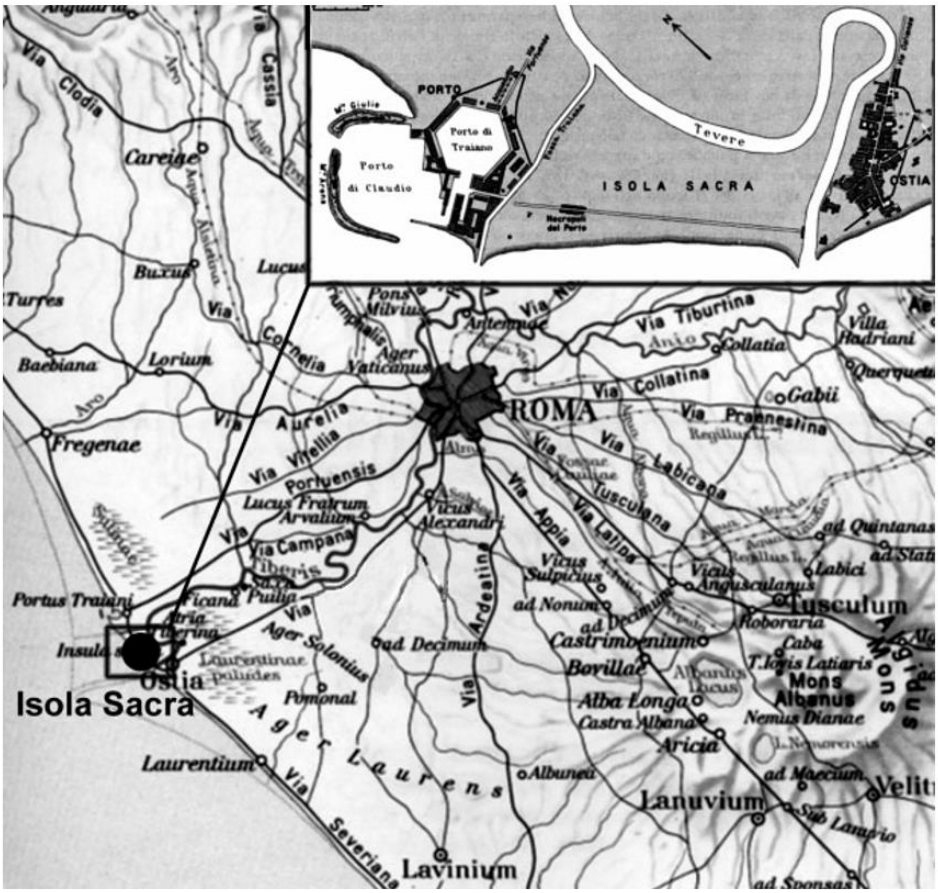

Figure 13: Map of Italy showing the position of Portus relative to Isola Sacra, Ostia, and Rome (from Prowse et al. 2007).

the impact that the regional environment had on the morbidity and mortality patterns at each site in the future.

Summary:

Collectively, the political-economic environment, prevalence of physical stress, residential infrastructure, and regional demography of the two cities help illuminate their significantly different age-specific mortality risks. After the stability and economic prosperity of the 2nd century, the inhabitants of Portus were faced with the consequences of political and economic instability throughout the 3rd century AD. In addition, this population had different residential quarters than at Petra, resulting in higher population density and its attendant issues of increased disease transmission and contact with human waste. The paleopathology data in fact indicates that Portus' inhabitants experienced frequent non-specific physiological stress during their lifetime, particularly in childhood, and forthcoming research suggests that vitamin D deficiency may have played a role in shaping mortality risk (Prowse personal communication). General physical stress, periodic food shortages, and/or infectious disease may be responsible for the overwhelming presence of DEHs in the larger sample. Additionally, as Portus lies in the malarial belt, malaria may have been one source in particular that was responsible for the pervasive levels of non-specific stress evinced in the paleopathological data (Prowse 2001; Scheidel 2003). The pervasiveness of non-specific stress at Portus could have directly lead to higher rates of age-specific mortality risk through increased frailty. The high prevalence of non-specific stress appears to correlate with the relatively young age (20-25 years) at which mortality climaxes in Portus.

In contrast, the residents of Petra lived during a fairly stable period in the Nabataean Kingdom's history which was characterized by political expansion and economic prosperity. Current archaeological data indicates that this population lived in a less densely settled urban

environment situated within a broader region whose population was more dispersed. Paleopathological and dietary data further suggests that this population had stable access to a nutritional diet and experienced a relatively low prevalence of physical stress in the form of malnutrition and/or infectious disease. The North Ridge population's political-economic environment, diet, urban environment, and regional environment may thus begin to explain the relatively low levels of age-specific mortality risk exhibited in this population.

Chapter 6: Conclusion

Cementochronology successfully met the challenge presented by the PNRP skeletal collection. Despite the commingled and fragmented nature of the sample, an adequate number of age-at-death estimates were able to be collected in order to proceed with an analysis of the age-at-death distribution and the age-specific mortality risk. Although the mortality rates may be considered high my modern standards, they fall outside the expectations for pre-industrial, urban populations. Indeed, the higher life expectancy, as demonstrated in the age-at-death distribution, suggest that the inhabitants at Petra were living longer than their urban counterparts in the broader Mediterranean region.

The comparison between the cemetery population of Portus and the North Ridge population confirms that Petra experienced significantly lower age-specific mortality rates compared to other contemporaneous populations. The examination and comparison of the political, economic, and social environments of Petra and Portus suggest that the prosperous political-economic environment, access to an adequate diet, and the less densely settled urban and regional environment of the North Ridge population may begin to explain the lower rates of non-specific stress and age-specific mortality exhibited by this population.

These results also help strengthen the conclusions of previous research on the North Ridge population. The high proportion (40%) of individuals aged 50 and higher agrees with the paleopathological data which revealed that activity and age related degenerative diseases were the most prevalent paleopathological conditions in the North ridge population (Canipe 2014). These results further suggest that the prevalence of infectious disease and malnutrition was relatively low among the North Ridge population. The age-at-death distribution argues against the presence of virulent diseases with high fatality rates which would result in a catastrophic model of mortality.

However, populations can still suffer from periods of prevalent physical stress and maintain an attritional pattern of mortality. Indeed, short periods of stressful events such as famine, adverse climatic change, exposure to new diseases, and harsh working conditions can all produce elevated attritional patterns of mortality (Chamberlain 2006).

Due to this, the possibility of a high prevalence of infectious disease cannot be completely ruled out. However, when all the bioarchaeological data is considered together, including the high percentage of older aged individuals, the lower rates of age-specific mortality risk, and the stable isotopic evidence for a nutritionally sound diet in combination with the low prevalence of paleopathological indicators, a stronger argument can be made for interpreting the paleopathological data as indicative of low prevalence of physical stress resulting from malnutrition and infectious disease for this portion of Petra's population.

The lower rates of mortality risk observed for the Petra North ridge population has further implications concerning general assumptions regarding mortality in the past. Although the age-specific risk of mortality might be considered relatively high by today's standards, it is notably lower than other archaeological populations, such as Portus. This is particularly so for pre-industrial, urban populations where the mortality risk resulting from infectious disease is assumed to have been high (Larsen 2015).

Before the industrial revolution, the expectation of life is generally estimated to have been short, less than 40 years for many (Gage et al. 2012). However, few modern countries share this short life expectancy at birth regardless of their state of economic development (Gage et al. 2012). When compared to modern day non-industrial populations, such as hunter-gathers, life expectancies for archaeological populations often fall below those for these modern non-industrial populations as well (Gage et al. 2012).

The trend of high mortality rates in the archaeological record have increasingly been met with skepticism. The underestimation of age due to bioarchaeological age estimation methods is a prevalent issue in paleodemographic studies (Bocquet Appel and Masset 1982; Chamberlain 2006; Gage et al. 2012). In addition to life expectancies for archaeological populations falling below that of modern non-industrial populations, age-at-death estimates derived from traditional bioarchaeological methods often make it appear as if that few individuals lived past the age of 60, although historic records indicate that this was not the case (Bocquet-Appel and Masset 1982). Reanalyzes of previous paleodemographic data using updated statistical methods have shown that when the biases of age estimations are controlled for, life expectancy for paleodemographic populations do indeed fall well within the range of modern non-industrial populations (Konigsberg and Hermann 2006). The results of this study further support the need to continue to question our assumptions about mortality in the past and try to correct for the error in age estimation methods.

Another important point of emphasis is the contextually dependent determinants of mortality risks. As already stated above, mortality risk is a complicated subject that is informed by a multitude of variables. For archaeological populations, many of these variables cannot be analyzed or can only be discussed somewhat superficially. The limitations of what can be discerned through archaeological, historical, and bioarchaeological research ensure that detailed analyses of mortality in paleodemographic populations will always be somewhat limited. However, in order to better understand patterns of mortality in the past and how they developed throughout time, more focus needs to be directed on trying to understand the specific contextually dependent variables that may be influencing a populations mortality and how they develop through time. By doing so a greater understanding of what the principal drivers behind mortality risk are, how they have influenced broad patterns of mortality risk throughout time, and perhaps most

importantly how they differ between different groups within a population to create biological inequalities can develop.

There is much research still to be done. Due to the subsequent excavations of shaft tombs on the North Ridge by the Petra North Ridge Project, the paleopathological and dietary data for the North Ridge population no longer covers the entirety of the PNRP skeletal collection. Both of these analyses need to be expanded in the future for a more detailed understanding of these variables and how they relate to mortality risk. In doing so, the contents of this analysis may either be strengthened or change dramatically. Expanding these analyses will also allow for a comparison of the similarities and differences between the different communities represented by the tombs. Currently, any heterogeneity that might allow for an intra-site comparison and a greater understanding of the different tomb populations are hidden behind small sample sizes and limited data.

Currently, the Petra North Ridge population only represents one particular portion of Petraean society during a circumscribed period. Due to this, the analysis is limited and significant differences between different segments of Petra's population and how they might differ over time cannot be determined. Data for the North Ridge population currently suggest that at least one portion of Petra's society may have benefited from their environment and experienced relatively low rates of physical stress in the form of malnutrition and infectious disease. However, this may not be the case for all of Petra's inhabitants. It is also difficult to assess the socio-economic status of the North Ridge population in relation to other segments of Petra's population due to the lack of bioarchaeological information available for skeletal assemblages collected outside the North Ridge. The expansion of bioarchaeological analysis to those skeletal assemblages that represent

various socio-economic classes in Petra would greatly contribute to our knowledge about Petra's inhabitants and how their experiences may have differed.

Expanding the use of cementochronology to other cemetery populations in the region would provide more comparative samples. The current analysis is hindered due to the use of differing methods of age-at-death estimation which prevents a comprehensive comparison of the North Ridge population to others in the same region. It is therefore unclear whether the patterns of mortality risk for this portion of Petraean society was exceptional for this period and region, or whether it is similar to other populations at the time. The paleopathological and dietary data suggest that although Petra is unique in some respects, the patterns exhibited among this population are similar to others in the region.

This study is also limited by the experience of the author. Cementochronology is not an intuitive method, but rather one that requires training. As this is the first time this author has used cementochronology as an age-at-death estimation method, intraobserver error may have introduced bias into the study. Although the results of this study appear to correlate well with previous research and what might be expected from the political, economic, and socio-cultural context for this sample, further work with cementochronology and a reevaluation of the age-at-death estimations should be pursued.

The results from this study suggest that the North Ridge population did not greatly suffer from the environmental stressors often assumed to have affected urban populations. In contrast, the age-at-death data suggests that this portion of Petra's population was living longer on average than their urban, rural/agricultural, and nomadic counterparts both in the Near East and in the broader Mediterranean region. The comparative analysis between the populations of Petra and Portus suggest that political, economic, social, and physical environment that the North Ridge

population shaped and navigated created prosperous conditions that may have helped thwart the contraction and transmission of infectious diseases that are often thought to have greatly burden pre-industrial cities and thus resulted in a lower age-specific risk of mortality than might be expected. Knowledge of the patterns and rates of mortality risk for the North Ridge population helps inform the analysis of other bioarchaeological topics of study such as diet and paleopathology. Because mortality is shaped by a multitude of variables and processes, further bioarchaeological research on the PNRP skeletal data will continue to contribute to our knowledge about the processes that molded mortality for this population and allow for more nuanced and informed interpretations in the future.

REFERENCES

Al-Bashaireh, K. and Al-Muheisen, Z. (2011). Subsistence Strategies and Paleodiet of Tell al-Husn, Northern Jordan: Nitrogen and Carbon Stable Isotope Evidence and Radiocarbon Dates. *Journal of Archaeological Science* 38(1): 2606-2612.

AlQahtani, S. J., Hector, M. P., and Liversidge, H. M. (2010). Brief communication: The London atlas of human tooth development and eruption. American Journal of Physical Anthropology 142(3): 481–490.

Al-Salameen, Z. (2011). The nabataeans and Asia minor. *Mediterranean Archaeology and Archaeometry* 11(2): 55–78.

Al-Shorman, A. (2004). Stable Carbon Isotope Analysis of Human Tooth Enamel from the Bronze AGe Cemetery of Ya'amoun in Northern Jordan. *Journal of Archaeological Science* 31(1): 1693-1698.

Anderson, B. (2002). Imperial Legacies, Local Identities: References to Achaemenid Perisan Iconography on Crenelated Nabataean Tombs. *Ars Orientalis* 32: 163–207.

Appleton, L. (2015, July). Dietary Reconstruction of Urban Inhabitants of the 1st Century AD Petra (Master's thesis). East Carolina University, Greenville, NC.

Aufderheide, A., Carmell, C., Zlonis, M., and Horne, P. (2003). Chemical dietary reconstruction of Greco-Roman mummies at Egypt's Dakhleh oasis. *Journal of the Society for the Study of Egyptian Antiquities* 30(1): 1-8.

Bairoch, P. (1989). Urbanization and the economy in preindustrial societies: the findings of two decades of research. *Journal of European Economic History* 18: 239-90.

Baldassare, I. (1990). Nuove ricerche nella necropoli dell'Isola Sacra. *Quaderni di Archeologia Etrusco-Italica,* 19: 164-172.

Barrett, R., Kuzawa, W., McDade, T., and Aremlagos, G. (1998). Emerging and Re-Emerging Infectious Diseases: The Third Epidemiologic Transition. *Annual Review of Anthropology* 27: 247-271.

Bartlett, M. (1957). Measles periodicity and community size. *J. R. Stat. Soc [Series A]* 120: 48-60.

Bazelmans, C., Henauw, S., Mattys, C., Dramaix, M., Kornitzer, M., Backer, G., and Leveque, A. (2006). Healthy Food and Nutrient Index and All Cause Mortality. *European Journal of Epidemiology* 21(2): 145-152.

Bengtsson, T. (1999). The Vulnerable Child. Economic Insecurity and Child Mortality in Pre-Industrail Sweden: A Case Study of Vastanfors, 1757-1850. *European Journal of Population* 15(2): 117-151.

Bengtsson, T., Campbell C., and Lee J.Z. (Eds.). (2004). *Life under pressure: Mortality and Living Standards in Europe and Asia, 1700-1900*. Cambridge, MA: The MIT Press.

Bikai, P., and Perry, M. (2001). Petra North Ridge Tombs 1 and 2: Preliminary Report. *Bulletin of the American Schools of Oriental Research* 324: 59–78.

Black, F. (1966). Measles endemicity in insular populations: critical community size and its evolutionary implications. *Journal of Theoretical Biology* 11: 207-211.

Bocquet-Appel, J., and Masset, C. (1982). Farewell to Paleodemography. *Journal of Human Evolution* 11: 321–333.

Bosshardt, D. and Selvig, A.K. (2000). Dental cementum: the dynamic tissue covering of the root. *Periodontology* 13: 41-75.

Bowersock, G.W. (1983). *Roman Arabia*. Cambridge, MA: Harvard University Press.

Bowersock, G. W. (2003). The Nabataeans in Historical Context. In *Petra Rediscovered: The Lost City of the Nabataean Kingdom* (pp. 19-26). New York: Harry N. Abrams.

Brickley, M. and Ives, R. (2008). *Bioarchaeology of Metabolic Bone Disease.* New York: Academic Press.

Brunt, P. (1971). *Italian manpower: 225 BC to AD 14.* New York: Oxford University Press.

Buikstra, J., and Ubelaker, D. (Eds.). (1994). *Standards for Data Collection from Human Skeletal Remains: Proceedings of a Seminar at the Field Museum of natural History. Arkansas: Arkansas Archeological Survey.*

Campbell, Lee, and Bengtsson, T. (2004). Economic Stress and Mortality. In *Life under pressure: mortality and living standards in Europe and Asia, 1700-1900* (pp. 61–78). Cambridge, Mass: MIT.

Canipe, C. (2014). *Exploring Quality of Life at Petra Through Paleopathology* (Master's thesis). East Carolina University, Greenville, NC.

Chamberlain, A. T. (2000). Problems and prospects in paleodemography. In *Human Osteology in Archaeology and Forensic Science* (pp. 101–115). Cambridge, UK: Cambridge University Press

Chamberlain, A. T. (2006). *Demography in archaeology*. Cambridge: Cambridge University Press.

Charles, D., Condon, K., Cheverud, J., and Buikstra, J. (1986). Cementum Annulation and Age Determination in Homo Sapiens. I. Tooth Variability and Onbserver Error. *American Journal of Physical Anthropology* 71: 311–320.

Chen L., Huq E., and D'Souza S. (1981). Sex bias in the family allocation of food and health care in rural Bangladesh. *Population and Development Review* 7: 55-71.

Cho, H. (2002). *Age-Associated Bone Loss in an Imperial Roman Population: An Histological Analysis of Inter-Skeletal and Intra-Skeletal Variability.* (Unpublished Ph.D. Dissertation). University of Missouri-Columbia. Columbia, Missouri.

Cohen, M. N. (1989). *Health and the rise of civilization*. New Haven: Yale University Press.

Croke, K. (2012). The Political Economy of Child Mortality Decline in Tanzania and Uganda, 1995-2007. *Studies in Comparative International Development* 46(4): 441-463.

Crooks, D. (1998). Poverty and Nutrition in Eastern Kentucky: The Political Economy of Childhood Growth. In Alan Goodman and Thomas Leatherman (Eds.), *Building a New Biocultural Synthesis: Political-Economic Perspectives on Human Biology* (pp. 339-358). Ann Arbor: University of Michigan Press.

Defo, B. (1996) Areal and socioeconomic differentials in infant and child mortality in Cameroon. *Soc. Sci. Med.*, 42: 399-420.

Defo, B. (2014). Beyond the "transition" frameworks: the cross-continuum of health, disease and mortality framework. *Global Health Action* 7: 1–16.

DeNiro, M., Epstein, S. (1981). Influence of diet on the distribution of nitrogen isotopes in animals. *Geochimica et Cosmochimica Acta* 45: 341-351.

DeWalt, B. (1998). The Political Ecology of Population Increase and Malnutrition in Southern Honduras. In Alan Goodman and Thomas Leatherman (Eds.), *Building a New Biocultural Synthesis: Political-Economic Perspectives on Human Biology* (pp. 295-316). Ann Arbor: University of Michigan Press.

DeWitte, S.N. and Wood, J.W. (2008). Selectivity of the Black Death with respect to preexisting health. *Proc. Natl. Acad. Sci. U.S.A.* 105: 1436-1441.

DeWitte, S., Boulware, J., and Redfern, R. (2013). Medieval Monastic Mortality: Hazard Analysis of Mortality Differences Between Monastic and Nonmonastic Cemeteries in England. *American Journal of Physical Anthropology* 152: 322–332.

Farmer, P. (1996). Social inequalities and emerging infectious diseases. *Emerging Infectious Diseases* 2: 259-69.

Fenner, F. (1970). The effects of changing social organization on the infectious diseases of man. In Stephen Boyden (ed.), *The Impact of Civilization on the Biology of Man* (pp. 48–76). Canberra: Australian National University Press.

Fiema, Z.T. (2003). Roman Petra (A.D. 106-363): A Neglected Subject. In *Zeitshcrift des Deutchen Palastina-Vereins* (vol 119, pp. 38-58). Weisbaden: Harrassowitz Verlag.

Floud, R., Wachter, K., and Gregory, A. (1990). *Height, Health, and History*. Cambridge, UK: Cambridge University Press.

Fogel, R. (2004). *The Escape from Hunger and Premature Death, 1700-2100: Europe, America, and the Third World*. Cambridge, UK: Cambridge University Press.

Gage, T.B. (1988). Mathematical hazard models of mortality: An alternative to model life tables. *American Journal of Physical Anthropology* 76(4): 429–441.

Gage, T.B. (1989). Bio-mathematical approaches to the study of human variation in mortality. *Yearbook of Physical Anthropology* 32: 185–214.

Gage, T.B, DeWitte, S., and Wood, J. (2012). Demography Part 1: Mortality and Migration. In Sara Stinson, Barry Bogin, and Dennis O'Rourke (Eds.), *Human Biology: An Evolutionary and Biocultural Perspective* (2nd ed., pp. 695–755). Hoboken, N.J.: John Wiley & Sons.

Gage, T.B, and Dyke, B. (1986). Parameterizing abridged mortality tables: the Siler three-component hazard model. *Human Biology* 58: 275–291.

Gage, T.B., and O'Connor, K. (2009). Nutrition and the Variation in Level and Age Patterns of Mortality. *Human Biology* 81(5/6): 551–574.

Gavrilov, L., and Gavrilova, N. (1991). *The biology of the life span: a quantitative approach*. London: Harwood Academic Publishers.

Geusa, G., Bondioli, L., Capucci, E., Cipriano, A., Grupe, G., Savore, C., and Macchiarelli, R. (1999). Osteodental biology of the people of Portus Romae (necropolis of Isola Sacra, 2nd-3rd Cent. AD). II. Dental cementum annulations and age at death estimates. Digitial Archives of Human Paleobiology, 2. Museo Naz. "L. Pigorini" Rome (CD-ROM, E-LISA, Milano).

Gogte, V. D. (1999). Petra, the Periplus and ancient Indo-Arabian maritime trade. *ADAJ* 43: 299–304.

Gompertz, B. (1825). On the nature of the function expressive of the law of human mortality, and on a new mode of determining the value of life contingencies. *Philosophical Transactions of the Royal Society of London* (Series A) 115: 513–585.

Goodman, A.H. (1998). The Biological Consequences of Inequality in Antiquity. In Alan Goodman and Thomas Leatherman (Eds.), *Building a New Biocultural Synthesis: Political-Economic Perspectives on Human Biology* (pp. 147-170). Ann Arbor: University of Michigan Press.

Goodman, A., Armelagos, G., and Rose, J. (1980). Enamel Hypoplasias as Indicators of Stress in Three Prehistoric Populations from Illinois. *Human Biology* 52(3): 515-528.

Goodman, A. H., and Leatherman, T. L. (Eds). (1998). *Building a New Biocultural Synthesis: Political-Economic Perspectives on Human Biology*. Ann Arbor: University of Michigan Press.

Gowland, R., and Chamberlain, A. T. (2005). Detecting plague: paleodemographic characterisation of a catastrophic death assemblage. *Antiquity* 79: 146–157.

Graf, David. (1992). Nabataean settlements and Roman occupation in Arabia Petaea. In M. Zaghloul, K. 'Amr F, F. Zayadine, R. Nabeel, and N.R. Tawfiz (Eds.), *Studies in History and Archaeology of Jordan* (pp. 253-260). Amman: Department of Antiquities.

Graf, D., Bedal, L.A., Schmid, S., and Sidebotham, S. (2005). The Hellenistic Petra Project: Excavations in the Civic Center, Preliminary Report of the First Season, 2004. *Annual of the Department of Antiquities of Jordan* 49: 417–442.

Hodges, R. and Whitehouse, D. (1983). *Mohammed, Charlemagne and the origins of Europe: archaeology and the Pirenne Hypothesis.* London: Duckworth.

Holman, D. J. (2005). mle: A Programming Language for Building Likelihood Models, Version 2.1 ed. Seattle, WA.

Hoppa, R. (2002). Paleodemography: Looking Back and Thinking Ahead. In *Paleodemography: Age Distributions from Skeletal Samples* (pp. 9–28). Cambridge, MA: Cambridge University Press.

James, W., Milner, G., Harpending, M., and Weiss, K. (1992). The Osteological Paradox. *Current Anthropology* 33(4): 343–370.

Johnson, D. J. (1987). Nabataean trade: intensification and culture change (Unpublished Ph.D. Dissertation).

Joukowsky, M. (2001). Nabataean Petra. *Bulletin of the American Schools of Oriental Research* 324: 1.

Jowett, J. (1991). The Demographic Responses to Famine: The Case of China 1958-61. *GeoJournal* 23(2): 135-146.

King, M. (2001). *Analysis of diet in Byzantine Jordan: isotopic evidence in human dentine.* (Unpublished Master's thesis). University of Arkansas, Fayetteville, Arkansas.

Konigsberg, L., and Hermann, N. (2006). The Osteological Evidence for Human Longevity in the Recent Past. In *The Evolution of Human Life History* (pp. 267–306). Santa Fe, NM: School for Advanced Research Press.

Larsen, C. (1995). Biological Changes in Human Populations with Agriculture. *Annual Review of Anthropology* 24:, 185-213.

Larsen, C. (2002). Bioarchaoelogy: The Lives and Lifestyles of Past People. *Journal of Archaeological Research* 10(2): 119–166.

Larsen, C. (2015). *Bioarchaeology: Interpreting Behavior from the Human Skeleton* (2nd ed.). Cambridge, MA: Cambridge University Press.

Leatherman, T. (1998). Illness, Social Relations, and Household Production and Reproduction in the Andes of Southern Peru. In Alan Goodman and Thomas Leatherman (Eds.), *Building a New Biocultural Synthesis: Political-Economic Perspectives on Human Biology* (pp. 245-268). Ann Arbor: The University of Michigan Press.

Leatherman, T. (2005). Coco-colonization of diets in Yucatan. *Social Science and Medicine* 61(4): 833-846.

Losch, S., Moghaddam, N., Grosschmidt, K., Risser, D., and Kanz F. (2014). Stable isotope and trace element studies on gladiators and contemporary Romans from Ephesus (Turkey, 2nd and 3rd Ct. AD)-Implications for differences in diet. *PLOS ONE* 9(10): 1-17.

Makeham, W. (1860). On the law of mortality. *Journal of the Institute of Actuaries* 13: 325–358.

Mannucci, V., and Verduchi P. (1996). Il porto imperiale di Roma: le vicende storiche. In Vanni Mannucci (ed.), *Il Parco Archeologico Naturalistico del Porto di Traiano* (pp. 15-28). Rome: Gangemi Editore.

Manzi, G., Sperduti, A., and Passarello P. (1991). Behavior-induced auditory exostoses in imperial Roman society: Evidence from coeval urban and rural communities near Rome. *American Journal of Physical Anthropology* 85: 253-260.

Manzi, G., Santandrea, E., and Passarello, P. (1999). Discontinuity of Life Conditions at the Transition From the Roman Imperial Age to the Early Middle Ages: Example From

Central Italy Evaluated by Pathological Dento-Alveolar Lesions. *American Journal of Human Biology* 11: 327-341.

Mayer, J. D. (2000). Geography, ecology and emerging infectious diseases. *Social Science and Medicine* 50(7–8): 937–952.

Meiggs, R. (1973). *Roman Ostia.* Oxford: Clarendon Press.

Millar, F. (1993). *The Roman Near East, 31 B.C.-A.D. 337*. Harvard University Press.

Milner, G., Wood, J., and Boldsen, J. (2008). Advances in Paleodemography. In M. A. Katzenberg and S. R. Saunders (Eds.), *Biological Anthropology of the Human Skeleton* (2nd ed., pp. 561–60). Hoboken, NJ: John Wiley & Sons.

Mode, C., and Busby, R. (1984). An eight-parameter model of human mortality: the single decrement case. *Bulletin of Mathematical Biology* 44: 647–659.

Mode, C., and Jacobsen, M. (1984). A parametric algorithm for computing model period and cohort human survival functions. *International Journal of Bio-Medical Computing* 15:, 341–356.

Morse, S. (1995). Factors in the emergence of infectious diseases. *Emerging Infectious Diseases* 1(1): 7–15.

Mouton, M. (2006). Les plus anciens monuments funeraires de Petra: une tradition de l'Arabie Preislamique. *Topoi Orient-Occident* 14(1): 79–119.

Naji, S., Colard, T., Blondiaux, J., Betrand, B., d'Incau, E., and Bocquet-Appel, J.P. (2016). Cementochronology, to cut or not to cut? *International Journal of Paleopathology* 140: 1-7.

Negev, A. (1977). The Nabataeans and the Provincia Arabia. In H. Temporini and W. Haase (Eds.), *Aufstieg und Niedergange der Romanishcen Welt* (Vol. 2, pp. 520–586). Berlin.

Oleson, J. P. (2007). Nabataean Water Supply, Irrigation and Agriculture. In Konstantinos D. Politis (Ed.), *The World of the Nabataeans Volume of the International Conference: The World of Herods and the Nabataeans held at the British Museum, 17-19 April 2001* (pp. 217–250).

Orenstein, W., and Gay, N. (2004). The Theory of Measles Elimination: Implications for the Design of Elimination Strategies. *Journal of Infectious Diseases* 189: S27-S35.

Ortner, D. J. (2003). Identification of Pathological Conditions in Human Skeletal Remains (2nd ed.). San Diego: Academic Press.

Parker, T., and Perry, M. (2013). Petra North Ridge Project: The 2012 Season. *Annual of the Department of Antiquities of Jordan.*

Parr, P. (1970). A Sequence of Pottery from Petra. In J. A. Sanders (Ed.), *Essays in Honor of Nelson Glueck, Near Eastern Archaeology in the Twentieth Century* (pp. 348–381). New York: Doubleday.

Parr, P. (2003). The Origins and Emergence of the Nabataeans. In Glenn Markoe (Ed.), *Petra Rediscovered: The Lost City of the Nabataean Kingdom* (pp. 27-36). New York: Harry N. Abrams.

Parr, P. (2007). The Urban Development of Petra. In Konstantinos Politis (ed.), *The World of the Nabataeans. Vol 2 of the International Conference The World of Herods and the Nabataeans held at the British Museum, 17-19 April, 2001* (Vol 2., pp. 273-300). Franz Steiner Verlag.

Pavolini, C. (1986). *La vita quotidiana a Ostia*. Bari: Laterza

Perry, M. (2002). *Health, labor, and political economy: A bioarchaeological analysi of three communities in Provinica Arabia* (Unpublished Ph.D. Dissertation). University of New Mexico, Albuquerque, New Mexio.

Perry, M. (2016). New Light on Nabataean Mortuary Rituals in Petra. *SHAJ* 12: 385-398.

Petriaggi, R., Bonacci, G., Corbonara, A., Vittori, M., Vivarelli, M., and Vori P. (1995). Scavi a Ponte Galeria: nuove acquisizioni sull'acquedoto di Porto e sulla topografia del territorio Portuense. *Arch. Laz.* 12: 361-373.

Prowse, T. (2001). *Isotopic and Dental Evidence for Diet from the Necropolis of Isola Sacra (1st - 3rd Centuries AD), Italy.* (Unpublished Ph.D. Dissertation). McMaster University, Hamilton, Canada.

Prowse, T. (2017, June 25). Personal Communication. E-mail.

Prowse, T., Schwarcz, H., Saunders, S., Macchiarelli, R., and Bondioli, L. (2004). Isotopic paleodiet studies of skeletons from the Imperial Roman-age cemetery of Isola Sacra, Rome, Italy. *Journal of Archaeological Science* 31: 259–272.

Prowse, T., Schwarcz, H., Garnsey, P., Knyf, M., Macchiarelli, R., and Bondioli, L. (2007). Isotopic Evidence for Age-Related Immigration to Imperial Rome. *American Journal of Physical Anthropology* 132: 510-519.

Robinson, O. (1992). *Ancient Rome: city planning and administration.* New York: Routledge.

Sachet, I. (2005). Etude sur le developpement et l' organisation des necropoles de Petra et Medain Salih. In *Deuxiemes rencontres doctorales d'Orient-Express. Actes du colloque tenu a Paris les 5,6, et 7 fevrier* (pp. 25–41). Paris: COREP.

Sandias, M. (2011). The Reconstruction of Diet and Environment in Ancient Jordan by Carbon and Nitrogen Stable Isotope Analysis of Human and Animal Remains. In Steven Mithen and Emily Black (Eds.), *Water, Life and Civilisation: Climate, Environment and Society in the Jordan Valley* (pp. 337-346). Cambridge: Cambridge University Press.

Santos, R., and Coimbra, C. (1998). On the (Un) Natural History of the Tupi-Monde Indians: Bioanthropology and Change in the Brazilian Amazon. In Alan Goodman and Thomas Leatherman (Eds.), *Building a New Biocultural Synthesis: Political-Economic Perspectives on Human Biology* (pp. 269-294). Ann Arbor: University of Michigan Press.

Scheidel, W. (2003). Germs for Rome. In C. Edwards and G. Woolf (Eds.), *Rome the cosmopolis* (pp. 158-176). Cambridge: Cambridge University Press.

Schmid, S. (2002). From Aretas to the Annexation: Petra and the Nabataeans. In J. Frosen and Z. T. Fiema (Eds.). *Petra: A City Forgotten and Rediscovered*, (pp. 44–59). Helsinki.

Schmid, S. (2008). The Hellenistic Period and the Nabataeans. In *Jordan: An Archaeological Reader* (pp. 353–412). London: Equinox.

Scrimshaw, N.S. (2000). Infection and nutrition: synergistic interactions. In KG Kiple and KC Ornelas (Eds.), *The Cambridge World History of Food* (pp. 1397-1411). Cambridge, UK: Cambridge University Press.

Sommer, A. and Loewenstein, M.S. (1975). Nutritional status and mortality. *American Journal of Clinical Nutrition* 28: 287-292.

Stambaugh, J. (1988). *The ancient Roman city.* Baltimore: Johns Hopkins University Press.

Stein, T. and Corcoran, J. (1994). Pararadicular cementum deposition as a criterion for age estimation in human beings. *Oral Surg Oral Med Oral Pathox* 77: 266–70.

Stott, G., Sis, R., and Levy, B. (1982). Cemental Annulation as an Age Criterion in Forensic Dentistry. *J. Dent Res* 61(6): 814–817.

Storey, G. (1997). The population of ancient Rome. *Antiquity* 71: 966-978.

Storey, G. (2001). Regionaries-Type 1: Architectural/Residential Units at Ostia. *American Journal of Archaeology* 105(3): 389-401.

Storey, G. (2002). Regionaries-Type Insulae 2: Architectural/Residential Units at Rome. *American Journal of Archaeology* 106(3): 411-434.

Swedland, A., and Ball, H. (1998). Nature, Nurture, and the Determinants of Infant Mortality: A Case Study from Massachusetts, 1830-1920. In Alan Goodman and Thomas Leatherman (Eds.), *Building a New Biocultural Synthesis: Political-Economic Perspectives on Human Biology* (pp. 191-228). Ann Arbor: University of Michigan Press.

Touzeau, A., Amiot, R., Blichert-Toft, J., Flandrois, J., Fourel, F., Grossi, C., Martineau, F., Richardin, P., and Christophe, L. (2014). Diet of Ancient Egyptians Inferred from Stable Isotope Systematics. *Journal of Archaeological Science* 46(1): 114-124.

Wadeson, L. (2012). The funerary landscape of Petra: results from a new study. In *The Nabataeans in Focus: Current Archaeological Research at Petra (Vol. 42).* Oxford: Archaeopress.

Walker, P., Bathurst, R., Richman, R., Gjerdrum, T., and Andrushko, V. (2009). The Causes of Porotic Hyperstosis and Cribra Orbitalia: A Reappraisal of the Iron-Deficiency-Anemia Hypothesis. *American Journal of Physical Anthropology* 139: 109-125.

Walker, P. L., Johnson, J. R., and Lambert, P. M. (1988). Age and sex biases in the preservation of human skeletal remains. *American Journal of Physical Anthropology* 76(2): 183–188.

Wenning, R. (2007). The Nabataeans in History. In Konstantinos Politis (Ed.), *The World of the Nabataeans: Vol 2 of the International Conference The World of the Herods and the Nabataeans held at the British Museum, 17-19 April, 2001* (Vol. 2, pp. 25–37). Franz Steiner Verlag.

White, C., and Armelagos, G. (1997). Osteopenia and stable isotope ratios in bone collagen of Nubian female mummies. *American Journal of Physical Anthropology* 103(2): 185-199.

White, C., Longstaffe, F., and Law, K. (1999). Seasonal stability and variation in diet as reflected in human mummy tissues from the Kharga Oasis and the Nile Valley. *Palaeogeography, Palaeoclimatology, Palaeoecology* 147(3): 209-222.

White, T., Black, M., and Folkens, P. (2012). *Human Osteology* (3rd Ed.). New York: Elsevier Academic Press.

Wittwer-Backofen, U., Gampe, J., and Vaupel, J. (2004). Tooth Cementum Annulation for Age Estimation: Results From a Large Known-Age Validation Study. *American Journal of Physical Anthropology* 123: 119–129.

Wood, J. (1998). A Theory of Preindustrial Dynamics: Demography, Economy, and Well-Being in Malthusian Systems. *Current Anthropology* 39(1): 99-135.

Wood, J., Holman, D., O'Connor, and Ferrell, R. (2002). Mortality Models of Paleodemography. In *Paleodemogrpahy: Age Distributions from Skeletal Samples* (pp. 129–170). New

York: Cambridge University Press.

Wood, J., Holman, D., Weiss, K., Buchanan, A., and LeFor, B. (1992). Hazards Models for Human Population Biology. *Yearbook of Physical Anthropology* 35: 43–87.

Wood, J., Milner G.R., Harpending, H.C., and Weiss, K.M. (1992) The Osteological Paradox. *Current Anthropology* 33(4): 343-370.

Yaussy, S.L., DeWitte, S.N., and Redfern, R.C. (2016). Frailty and famine: Patterns of mortality and physiological stress among victims of famine in medieval London. *American Journal of Physical Anthropology* 160(2): 272-283.

Zeitler, J.P. (1990) A Private Building from the First Century BC in Petra. *ARAM* 2: 385-420.

Zuckerman, M. K. (2012). Evolutionary Thought in Paleopathology and the Rise of the Biocultural Approach. In *A Companion to Paleopathology* (pp. 34). Malden, MA: Blackwell Publishing.

Appendix A: Sample breakdown and age-at-death estimates

Project/Year	Context Number	Tooth Number	Individual Number	Tooth Type	M/M Number **	Crown Presence	TCA Mean †	Age-at-Death	Individual Age-At-Death	Rounded
PNRP12	B.4:10	1	1	RM1	2	complete	32	38.5	41.5	41.5
PNRP12	B.4:10	2	1	RM2	2	none	32	44.5		
PNRP12	B.4:17	8	2	RI_2	4	none	38.33	45.83	43.67	44
PNRP12	B.4:17	282	2	LC_1	4	none	32	41.5		
PNRP12	B.4:22	11	70	LPM2		none	51	61.5	61.5	61.5
PNRP12	B.4:22	10	3	RC ^		complete	54.67	66.17	63	63
PNRP12	B.4:17	6	3	LC ^	-	complete	47.33	59.83		
PNRP12	B.4:23	12	4	LM_1		complete	38.6	45.1	45.1	45
PNRP12	B.5:15	19	5	LI1	5	none	52.5	60	61	61
PNRP12	B.5:15	20	6	RI1	5	none	-	-		
PNRP12	B.5:15	22	5	RC	5	none	50	62		
PNRP12	B.5:15	25	6	RM2	6	none	23.5	36	34.42	34
PNRP12	B.5:15	26	6	RM1	6	none	25.33	32.83		
PNRP12	B.5:15	27	7	RPM2	6	none	19	31.5		
PNRP12	B.5:15	23	-	C1		none	16.67	29.17	-	
PNRP12	B.5:15	266	7	LPM_2	7	none	27	39.5	39.34	39
PNRP12	B.5:15	267	7	LM_1	7	partial	31.67	39.17		
PNRP12	B.5:15	262	8	LC	8	none	18.67	31.17	31.67	32
PNRP12	B.5:15	263	8	LPM_2	8	none	19.67	32.17		
PNRP12	B.5:17	29	9	LM_2		none	20.33	31.83	31.83	32
PNRP12	B.5:4	113	10	LPM_2		complete	54	65.5	65.5	65.5
PNRP14	B.5:33	39	11	LI2	56	none	39	48.5	48.5	48.5
PNRP14	B.5:32	34	12	LI1		partial	31	38.5	38.5	38.5
PNRP14	B.5:32	33	13	RI1		complete	45.33	52.83	52.83	53
PNRP12	B.5:0	17	14	I2		none	50	57.5	57.5	57.5
PNRP14	B.5:34	59	15	LM2	15	none	26.33	38.83	38.83	39
PNRP14	B.5:34	51	16	RPM2	12	complete	34.75	47.25	45.25	45

PNRP14	B.5:34	52	16	RPM1	12	complete	31.75	43.25		
PNRP14	B.5:34	46	17	RI2		none	46.25	53.75	53.75	54
PNRP14	B.5:34	47	18	PM2		none	13	25.5	25.5	25.5
PNRP14	B.5:35	99	19	LM_2	26	none	44	55.5	55.5	55.5
PNRP14	B.5:35	93	20	LM_1	31	none	33.57	40.07	39.05	39
PNRP14	B.5:35	94	20	LM_2	31	none	33.33	39.83		
PRNP14	B.5:35	97	20	RM_2	32	none	30.75	37.25		
PNRP14	B.5:35	90	21	RM_1	29	none	47.25	54.75	54.75	55
PNRP14	B.5:35	73	22	RPM_1	19	none	44.75	56.25	56.25	56
PNRP14	B.5:35	85	23	RM_2	23	none	26.5	38	38	38
PNRP14	B.5:35	72	24	LPM_2	18	none	44.33	56.83	55.44	55
PNRP14	B.5:35	82	24	RPM1	21	none	44	55.5		
PNRP14	B.5:35	83	24	RM2	21	none	41.5	54		
PNRP14	B.5:35	281	25	RI_2	22	none	21.33	28.83	30.83	31
PNRP14	B.5:35	280	25	RC	22	none	18	30.5		
PNRP14	B.5:35	105	25	RPM_2	22	none	20.67	33.17		
PNRP14	B.5:35	109	26	RC	25	none	51	63.5	65.665	66
PNRP14	B.5:35	110	26	RPM_1	25	none	56.33	67.83		
PNRP14	B.5:35	77	27	RC	20	partial	58	70.5	68	68
PNRP14	B.5:35	79	27	LI2	20	none	54	65.5		
PNRP12	B.5:31	283	28	LM_2	10	none	35	46.5	46.5	46.5
PNRP12	B.5:31	259	28	RM_2	10	none	35	46.5		
PNRP14	B.6:42	276	29	RPM2		complete	40.5	53	53	53
PNRP14	B.6:34	143	30	I2		none	45	55.5	55.5	55.5
PNRP12	B.6:6	183	31	RPM2		partial	23	34.5	36.5	36.5
PNRP12	B.6:6	184	31	PM_2		none	26	38.5		
PNRP12	B.6:10	135	32	RI1		complete	36.75	44.25	44.25	44
PNRP12	B.6:5	189	33	M_2		complete	38	49.5	49.5	49.5
PNRP12	B.6	118	34	RM_1		complete	22	28.5	28.5	28.5
PNRP14	B.6:37	147	35	RI2		complete	27.67	37.17	37	37
PNRP14	B.6:38	275	35	LI2		complete	27.33	36.83		
PNRP14	B.6:36	144	36	LI2		complete	31.67	41.17	41.17	41

PNRP14	B.6:44	167	37	LI2	43	none	51.5	59	63.33	63
PNRP14	B.6:44	168	37	LC	43	none	52	64.5		
PNRP14	B.6:44	160	37	LI1	43	none	59	66.5		
PNRP14	B.6:44	165	38	RM1	44	none	24.78	31.28	35.89	36
PNRP14	B.6:44	166	38	RM2	44	none	28	40.5		
PNRP14	B.6:43	151	39	LC	39	none	30.67	43.17	37.65	38
PNRP14	B.6:43	152	39	LPM1	39	none	20.66	32.16		
PNRP14	B.6:44	164	40	LM2	42	complete	15.67	28.17	28.17	28
PNRP14	B.6:31	140	41	RPM1	37	none	58	69.5	71.53	71.5
PNRP14	B.6:31	141	41	LC1		partial	56.75	69.25		
PNRP14	B.6:31	142	41	RI2		none	66.33	75.83		
PNRP14	B.6:43	154	42	LM2	40	none	23.333	36.83	36.83	37
PNRP14	B.6:28	132	43	RM2	36	complete	20.67	33.17	33.17	33
PNRP14	B.7:34	238	44	C		none	26.5	39	36.21	36
PNRP14	B.7:34	247	44	RC	55	none	24.67	37.17		
PNRP14	B.7:34	248	44	RPM1	55	none	23.33	34.83		
PNRP14	B.7:34	241	44	LPM1		none	22.33	33.83		
PNRP14	B.7:34	240	45	C1		none	54.5	67	67	67
PNRP14	B.7:20	205	46	LI_1		complete	51	57.5	58.5	58.5
PNRP14	B.7:20	202	46	RI_1		complete	52	59.5		
PNRP14	B.7:34	245	-	LPM_1		complete	24.33	35.83	35.83	
PNRP14	B.7:27	211	47	LM2		complete	42.33	54.83	54.83	55
PNRP14	B.7:27	210	48	LPM1		complete	32.5	44	44	44
PNRP14	B.7:19	192	-	RI2		complete	42.5	51	51	
PNRP14	B.7:19	199	49	LI_2		complete	40.67	47.17	47.17	47
PNRP14	B.7:19	194	50	RI_2		complete	13.2	20.7	20.7	21
PNRP14	B.7:19	195	51	LI2		complete	55	64.5	64.5	64.5
PNRP14	B.7:31	219	52	LPM_1		complete	40.6	52.1	52.1	52
PNRP14	B.7:31	222	53	LPM2	52	partial	34.8	47.3	47.3	47
PNRP14	B.7:33	228	54	LI_1		complete	31.75	38.25	38.25	38
PNRP14	B.7:33	235	55	LC1		complete	53.5	66	66.35	66
PNRP14	B.7:33	234	55	RC1		complete	54.33	66.7		

PNRP14	B.7:33	232	56	RI_2		complete	35.4	42.9	42.9	43
PNRP14	B.7:33	237	57	RI_2		complete	50.33	57.83	57.83	58
PNRP14	B.7:33	274	-	LI_1		complete	48.33	54.83	54.83	
PNRP14	B.7:31	272	58	RI_2		complete	35	44.5	44.5	44.5
PNRP14	B.7:32	226	-	RM_2	54	none	32	44.5	44.5	
Tomb 2	Tomb 2	251	59	RI1		complete	15	22.5	22.5	22.5
Tomb 2	Tomb 2	250	60	LI1		complete	57.33	64.83	64.83	65
Tomb 2	Tomb 2	257	61	RM_1		partial	25	36.5	36.5	36.5
Tomb 2	Tomb 2	258	62	LM_2		partial	43.5	56	56	56
PNRP16	F.1:28.115.S34	298	63	RPM_2		complete	15.67	28.17	28.17	28
PNRP16	F.1:28.97.69	312	64	RC1	57	complete	24.7	37.2	37.2	37
PNRP16	F.1:28.115.35	319	65	RPM1	58	complete	20.75	32.25	30.125	30
PNRP16	F.1:28.115.35	320	65	LI2	58	complete	19.5	28		
PNRP16	F.1:28.119.S1	292	66	LPM_1		complete	41	52.5	52.5	52.5
PNRP16	F.1:9.70	310	67	RPM2		complete	19.67	32.17	32.17	32
PNRP16	F.1:28.90.S1.bo	305	68	LPM1		complete	23	34.5	34.5	34.5
PNRP16	F.1:28.98.S1	307	69	LPM1		none	21	32.5	32.5	32.5
PNRP16	F.1:28.116.1	300	-	RI1		complete	18	30.5	30.5	

* The orange cells highlight the teeth that had no viable cementum and the red cells the teeth that were omitted due to double sampling.

** M/M number refers to the numbers given to the fragments of mandibles and maxillae.

† TCA refers to the tooth cementum annulation count. The TCA mean is the counts of cementum for each slide belonging to a particular tooth averaged together.

Appendix B: Atlas of Human Tooth Development and Eruption (Al-Qhatani 2010)

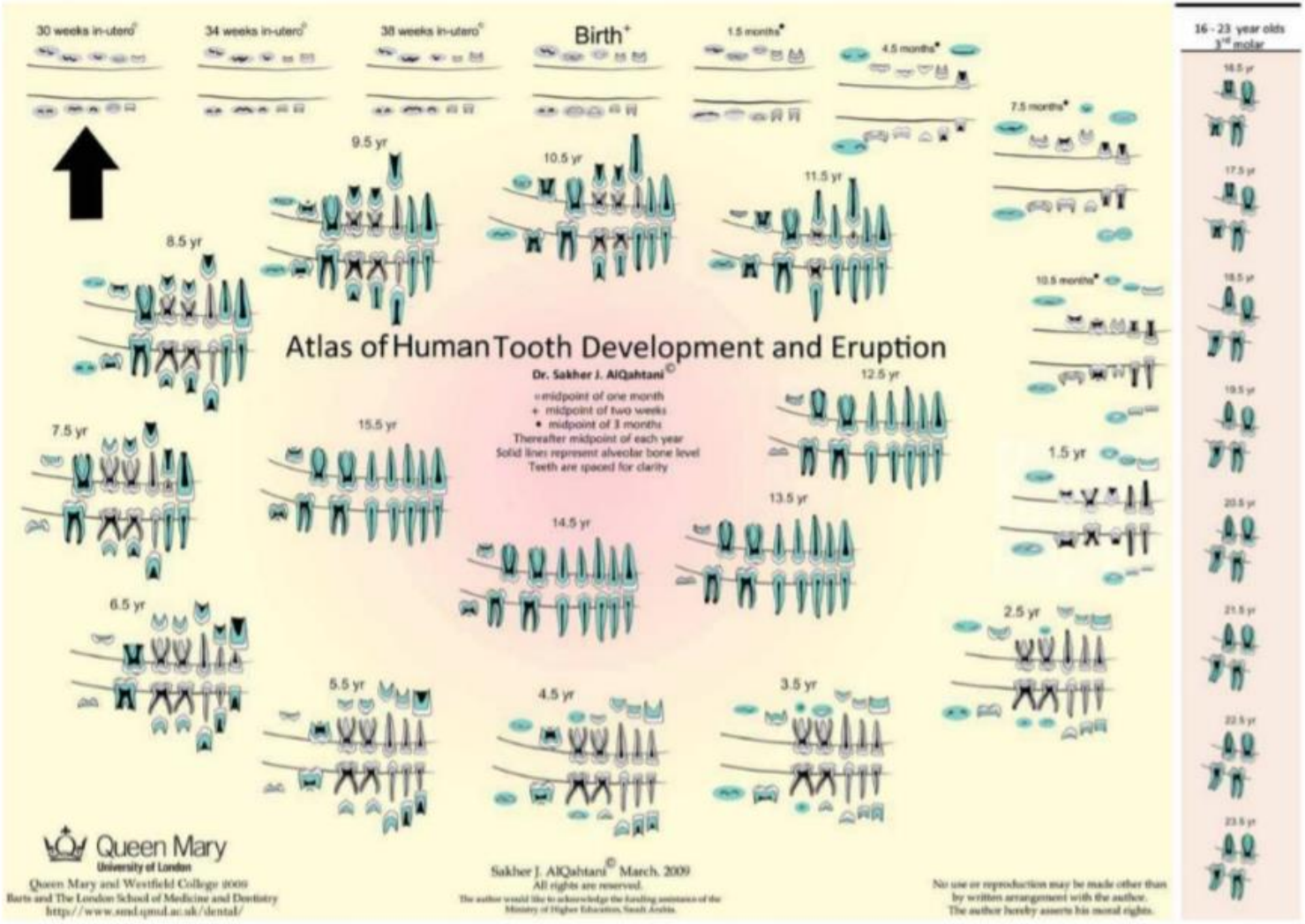

Fig. 6. Atlas of human tooth development and eruption. The arrow indicates the starting point. The dentine is presented in gray for deciduous teeth and in green for permanent.

Appendix C: Age-at-death estimates for Isola Sacra (Geusa et al. 1999)

Population	Individual	Tooth	Age-at-Death
Isola Sacra	SCR015	LLP3	52-55
Isola Sacra	SCR016	LRP3	43-46
Isola Sacra	SCRO18	LRP3	30-33
Isola Sacra	SCR019	URC	48-50
Isola Sacra	SCR027	LRP3	25-28
Isola Sacra	SCR037	LRP4	44-47
Isola Sacra	SCR038	ULP3	42-45
Isola Sacra	SCR038	LRP4	51-54
Isola Sacra	SCR039	LLP4	47-51
Isola Sacra	SCR039	LLP3	48-51
Isola Sacra	SCR044	LLP3	46-49
Isola Sacra	SCR044	ULP3	30-33
Isola Sacra	SCR055	URP4	49-52
Isola Sacra	SCR058	ULP4	21-24
Isola Sacra	SCR069	LRP4	39-43
Isola Sacra	SCR077	ULP3	41-44
Isola Sacra	SCR077	LRP4	40-43
Isola Sacra	SCR079	ULP3	44-47
Isola Sacra	SCR086	LLP3	19-22
Isola Sacra	SCR088	LLP3	35-38
Isola Sacra	SCR099	URP4	33-36
Isola Sacra	SCR097	ULP3	40-43
Isola Sacra	SCR099	LRP3	21-24
Isola Sacra	SCR105	URP3	32-35
Isola Sacra	SCR106	URP3	23-26
Isola Sacra	SCR118	URP4	38-41
Isola Sacra	SCR126	LLP4	19-22
Isola Sacra	SCR127	ULP3	27-30
Isola Sacra	SCR132	LRP4	25-29
Isola Sacra	SCR132	LLP4	30-34
Isola Sacra	SCR142	LRP3	28-31
Isola Sacra	SCR142	LLP3	28-31
Isola Sacra	SCR150	LLP4	42-46
Isola Sacra	SCR156	LRP4	40-44
Isola Sacra	SCR160	ULP3	36-39
Isola Sacra	SCR171	URP4	25-28
Isola Sacra	SCR172	LLP4	50-53
Isola Sacra	SCR174	URP3	30-33
Isola Sacra	SCR185	ULP3	41-44

Isola Sacra	SCR191	LLP4	32-35
Isola Sacra	SCR192	LLP4	27-30
Isola Sacra	SCR193	URP3	26-29
Isola Sacra	SCR217	URP3	32-35
Isola Sacra	SCR223	LRP4	25-29
Isola Sacra	SCR232	ULP4	38-41
Isola Sacra	SCR233	LLP4	42-46
Isola Sacra	SCR239	ULC	33-35
Isola Sacra	SCR245	LLP4	24-28
Isola Sacra	SCR250	ULP4	30-33
Isola Sacra	SCR251	LRP3	22-25
Isola Sacra	SCR252	LRP4	26-30
Isola Sacra	SCR256	LRP4	27-30
Isola Sacra	SCR257	ULP4	34-37
Isola Sacra	SCR258	LRP4	35-39
Isola Sacra	SCR272	URP3	24-27
Isola Sacra	SCR272	LLP3	24-27
Isola Sacra	SCR282	ULP4	30-33
Isola Sacra	SCR284	ULC	24-27
Isola Sacra	SCR285	LLP4	30-34
Isola Sacra	SCR285	LLP3	41-44
Isola Sacra	SCR286	URP3	33-36
Isola Sacra	SCR286	LLP3	38-41
Isola Sacra	SCR287	LLC	27-29
Isola Sacra	SCR287	LRP4	30-33
Isola Sacra	SCR288	LLP3	27-30
Isola Sacra	SCR288	LRP3	38-41
Isola Sacra	SCR289	LRP3	46-49
Isola Sacra	SCR294	ULC	56-58
Isola Sacra	SCR295	URP4	33-36
Isola Sacra	SCR296	LRP3	28-31
Isola Sacra	SCR297	ULP4	37-40
Isola Sacra	SCR298	URP3	32-35
Isola Sacra	SCR300	ULP3	52-55
Isola Sacra	SCR301	LRP3	39-42
Isola Sacra	SCR302	URP3	40-43
Isola Sacra	SCR305	ULC	24-26
Isola Sacra	SCR306	ULP3	24-27
Isola Sacra	SCR310	URC	23-26
Isola Sacra	SCR312	ULP3	38-41
Isola Sacra	SCR314	ULC	38-40
Isola Sacra	SCR316	URP3	35-38
Isola Sacra	SCR317	LLC	23-25
Isola Sacra	SCR324	ULC	36-38
Isola Sacra	SCR332	URC	32-34

Isola Sacra	SCR339	LRP3	42-45
Isola Sacra	SCR340	LRC	19-21
Isola Sacra	SCR343	URP4	24-27
Isola Sacra	SCR344	LLC	37-39
Isola Sacra	SCR352	URP3	24-27
Isola Sacra	SCR354	LLP4	22-25
Isola Sacra	SCR354	LRP4	21-24
Isola Sacra	SCR361	LRP3	22-25
Isola Sacra	SCR404	LLP3	23-26
Isola Sacra	SCR411	LRP3	25-28
Isola Sacra	SCR411	LRP4	23-27
Isola Sacra	SCR415	LLP3	23-26
Isola Sacra	SCR426	ULP3	24-27
Isola Sacra	SCR431	LLP3	39-42
Isola Sacra	SCR442	LRP4	18-22
Isola Sacra	SCR443	LLP3	47-50
Isola Sacra	SCR445	LRP4	28-32

Appendix D: mle Program (Holman 2005)

```
MLE
  TITLE = "PetraGM.mle.txt"
  DATAFILE("-.dat.txt")
  OUTFILE("-.out.txt")

  METHOD = SIMPLEX
  MAXITER = 5000
  EPSILON = 0.000001
  INTEGRATE_METHOD = I_ROMBERG

  EXP_HAZARD = TRUE
  maxage = 200


   DATA
     age              FIELD 1
   END {of data statement}

  END
  MODEL
     DATA
          PDF MAKEHAM (age, age, 20)    {this is the PDF}
               PARAM  a1  LOW = 0  HIGH = 1  START = 0.1   FORM = LOGLIN      END
               PARAM  a2  LOW = 0  HIGH = 1  START = 0.1   FORM = LOGLIN      END
               PARAM  b   LOW = 0  HIGH = 1  START = 0.1   FORM = LOGLIN      END
       END                  {end of pdf Makeham}
        END {of data}
```

```
  RUN
        FULL
        REDUCE a1 = 0.0
  END {of model}
END {of mle program}
```

Appendix E: Petra and Isola Sacra MLE output

Petra

70 lines read from file AllTombsGM.dat.txt

70 Observations kept and 0 observations dropped.

NAME age

MEAN 45.8714286

VAR 162.599172

STDEV 12.7514380

MIN 21.0000000

MAX 71.5000000

MonasticandNonGM.mle.txt

Program file: PetraGM.mle.txt

Input data file name: AllTombsGM.dat.txt

1 variables read.

Model 1 Run 1 : PetraGM.mle.txt

METHOD = SIMPLEX MAXITER = 5000 MAXEVALS = 100000

Convergence at EPSILON = 0.0000010000

LogLikelihood: -274.6189 AIC: 555.23778 Del(LL): 0.0000006818

Iterations: 289 Function evals: 402 Time: 00:00:00

Converged normally

Results with estimated standard errors. (28 evals)

Solution with 3 free parameters

Name	Form	Estimate	Std Error	t	against
a1	LOGLIN	0.000000003047	0.019263441155	0.00000015816	0.0
a2	LOGLIN	0.002720015668	0.005354142887	0.50802074689	0.0
b	LOGLIN	0.065051997231	0.032514628663	2.00069937460	0.0

Model 1 Run 2 : PetraGM.mle.txt

METHOD = SIMPLEX MAXITER = 5000 MAXEVALS = 100000

Convergence at EPSILON = 0.0000010000

LogLikelihood: -274.6189 AIC: 553.23778 Del(LL): 0.0000006565

Iterations: 48 Function evals: 85 Time: 00:00:00

Converged normally

Results with estimated standard errors. (19 evals)

Solution with 2 free parameters

Name	Form	Estimate	Std Error	t	against
a2	LOGLIN	0.002718932054	0.001530118793	1.77694180777	0.0
b	LOGLIN	0.065057533930	0.012050237952	5.39885885989	0.0

Isola Sacra

88 lines read from file IsolaSacraGM.dat.txt

88 Observations kept and 0 observations dropped.

NAME age

MEAN 34.3494318

VAR 82.1358330

STDEV 9.06288216

MIN 20.0000000

MAX 57.0000000

MonasticandNonGM.mle.txt

Program file: MonasticandNonGM.mle.txt

Input data file name: IsolaSacraGM.dat.txt

1 variables read.

Model 1 Run 1 : MonasticandNonGM.mle.txt

METHOD = SIMPLEX MAXITER = 5000 MAXEVALS = 100000

Convergence at EPSILON = 0.0000010000

LogLikelihood: -309.3828 AIC: 624.76556 Del(LL): 0.0000008167

Iterations: 107 Function evals: 174 Time: 00:00:00

Converged normally

Results with estimated standard errors. (27 evals)

Solution with 3 free parameters

Name	Form	Estimate	Std Error	t	against
a1	LOGLIN	0.019179036806	0.037830226505	0.50697652587	0.0
a2	LOGLIN	0.003082207527	0.008364160544	0.36850171767	0.0
b	LOGLIN	0.085202874637	0.054310285783	1.56881654015	0.0

Model 1 Run 2 : MonasticandNonGM.mle.txt

METHOD = SIMPLEX MAXITER = 5000 MAXEVALS = 100000

Convergence at EPSILON = 0.0000010000

LogLikelihood: -309.4737 AIC: 622.94746 Del(LL): 0.0000008020

Iterations: 39 Function evals: 71 Time: 00:00:00

Converged normally

Results with estimated standard errors. (18 evals)

Solution with 2 free parameters

Name	Form	Estimate	Std Error	t	against
a2	LOGLIN	0.008822077239	0.004156640278	2.12240575312	0.0
b	LOGLIN	0.064449748601	0.013289612022	4.84963357059	0.0

Appendix F: Differential Mortality MLE Program

```
MLE
  TITLE = "PetravNonGM.mle.txt"
  DATAFILE("-.dat.txt")
  OUTFILE("-.out.txt")

  METHOD = SIMPLEX
  MAXITER = 5000
  EPSILON = 0.000001
  INTEGRATE_METHOD = I_ROMBERG

  EXP_HAZARD = TRUE
  maxage = 120

   DATA
     age             FIELD 1   {estimated age at death}

                 FIELD 2


   END {of data statement}

END
  MODEL
     DATA

PDF MAKEHAM (age, age, 15)
{this is the PDF}
```

```
PARAM  a1  LOW = 0  HIGH = 1  START = 0.1  FORM = LOGLIN   END

PARAM  a2  LOW = 0  HIGH = 1  START = 0.1  FORM = LOGLIN
END

PARAM  b   LOW = 0  HIGH = 1  START = 0.1  FORM = LOGLIN
END

HAZARD COVAR population PARAM ha_population  LOW = -10 HIGH = 10 START = 0.0

END
      END                {end of pdf Makeham}

END {of data}
  RUN

FULL

REDUCE ha_population = 0.0

REDUCE a1 = 0.0

REDUCE ha_population = 0.0 a1 = 0.0
  END {of model}
END {of mle program}
```

Appendix G: Output of Petra vs. Isola Sacra

158 lines read from file PetravIsolaSacraGM.dat.txt

158 Observations kept and 0 observations dropped.

NAME	age	monastic
MEAN	39.4414557	0.55696203
VAR	149.367968	0.24832702
STDEV	12.2216189	0.49832421
MIN	20.0000000	0.00000000
MAX	71.5000000	1.00000000

MonasticvNonGM.mle.txt

Program file: PetravNonGM.mle.txt

Input data file name: PetravIsolaSacraGM.dat.txt

2 variables read.

Model 1 Run 1 : PetravNonGM.mle.txt

METHOD = SIMPLEX MAXITER = 5000 MAXEVALS = 100000

Convergence at EPSILON = 0.0000010000

LogLikelihood: -596.4848 AIC: 1200.9696 Del(LL): 0.0000007166

Iterations: 84 Function evals: 145 Time: 00:00:00

Converged normally

Results with estimated standard errors. (39 evals)

Solution with 4 free parameters

Name	Form	Estimate	Std Error	t	against
a1	LOGLIN	6.04225E-0010	0.005774422866	0.00000010464	0.0
a2	LOGLIN	0.001503624466	0.001531057384	0.98208237114	0.0
b	LOGLIN	0.077191109439	0.018515925288	4.16890369975	0.0
ha_population		1.221034491073	0.184758209975	6.60882399347	0.0

Model 1 Run 2 : PetravNonGM.mle.txt

METHOD = SIMPLEX MAXITER = 5000 MAXEVALS = 100000

Convergence at EPSILON = 0.0000010000

LogLikelihood: -619.1125 AIC: 1244.2251 Del(LL): 0.0000005601

Iterations: 56 Function evals: 102 Time: 00:00:00

Converged normally

Results with estimated standard errors. (30 evals)

Solution with 3 free parameters

Name	Form	Estimate	Std Error	t	against
a1	LOGLIN	0.000000001381	0.018957319858	0.00000007287	0.0
a2	LOGLIN	0.005700367463	0.007424502322	0.76777771977	0.0
b	LOGLIN	0.057015332678	0.021912695128	2.60193154449	0.0

Model 1 Run 3 : PetravNonGM.mle.txt

METHOD = SIMPLEX MAXITER = 5000 MAXEVALS = 100000

Convergence at EPSILON = 0.0000010000

LogLikelihood: -596.4848 AIC: 1198.9696 Del(LL): 0.0000008016

Iterations: 56 Function evals: 103 Time: 00:00:00

Converged normally

Results with estimated standard errors. (26 evals)

Solution with 3 free parameters

Name	Form	Estimate	Std Error	t	against
a2	LOGLIN	0.001503512070	0.000621571339	2.41888899445	0.0
b	LOGLIN	0.077195735033	0.008481932976	9.10119606568	0.0
ha_population		1.221114472449	0.183028644039	6.67171239159	0.0

Model 1 Run 4 : PetravNonGM.mle.txt

METHOD = SIMPLEX MAXITER = 5000 MAXEVALS = 100000

Convergence at EPSILON = 0.0000010000

LogLikelihood: -619.1125 AIC: 1242.2251 Del(LL): 0.0000007505

Iterations: 32 Function evals: 62 Time: 00:00:00

Converged normally

Results with estimated standard errors. (20 evals)

Solution with 2 free parameters

Name	Form	Estimate	Std Error	t	against
a2	LOGLIN	0.005700334592	0.001750025103	3.25728732753	0.0
b	LOGLIN	0.057013803046	0.007032473176	8.10721941146	0.0